CERN-TH.4473/86
MAD/TH/86-15
LBL-22861
UCB-PTH-87/3

SUPERSTRING MODELS CHALLENGED BY RARE PROCESSES

B.A. Campbell*), J. Ellis, K. Enqvist**), M.K. Gaillard***) and D.V. Nanopoulos**)

CERN-Geneva

ABSTRACT

Superstring models compactified on Calabi-Yau manifolds contain additional matter fields and gauge bosons beyond those in the Standard Model. The new matter and gauge couplings would make additional contributions to conventional electroweak processes, generate extra flavour-changing neutral interactions, and mediate new interactions leading to proton decay and neutrino masses. We use the phenomenological constraints on such effects to derive upper bounds on Yukawa couplings in low-energy dynamical models inspired by the superstring. We draw attention to the processes which give the best bounds on new Yukawa couplings, and which are those where novel superstring effects might first appear as experimental sensitivity is improved. Our bounds are not sufficient to exclude most superstring models with additional light particles, but do suggest that some couplings are too small to realize certain scenarios for symmetry breaking by radiative corrections.

---

*) Permanent address: Department of Physics, University of Alberta, Edmonton, Alberta, Canada.

**) Present address: Department of Physics, University of Wisconsin, Madison, Wis., USA.

***) Permanent address: LBL and Department of Physics, University of California, Berkeley, Calif., USA.

CERN-TH.4473/86
December 1986

1. INTRODUCTION

Although many theorists agree that the superstring [1] is a plausible candidate Theory of Everything (TOE), there is no consensus how to do phenomenology with it [2], and there are almost as many proposals as there are people working on the problem. One may hope that diligent theoretical analysis will ultimately reveal a unique consistent possibility for the low-energy limit of the superstring in four dimensions, although it could be that the present ambiguities in solving the theory will always persist. Either way, at the present time we must use experimental constraints to guide us towards the correct model for superstring phenomenology.

Historically, effects which are either rare or forbidden in the Standard Model have been very useful tools for constraining or excluding attempts to go beyond the Standard Model. These have included the absence of novel interactions causing baryon decay or neutrino masses, which were the nemesis of certain Grand Unified Theories (GUTs) [3]. One of the features of this paper is a reanalysis of proton decay and neutrino masses in the context of low-energy models inspired by the superstring. Important constraints on theoretical attempts to go beyond the Standard Model have also been provided by flavour-changing neutral interactions (FCNIs) [4]. They drove an important nail into the coffin of extended technicolour theories [5] but failed to rule out minimal supersymmetric [6] extensions of the Standard Model. In this paper we examine in detail the FCNIs in low-energy models inspired by the superstring, using phenomenological constraints on them to bound Yukawa couplings and to provide indications on the possible low-energy gauge group.

Phenomenological low-energy theories inspired by the superstring in general contain additional matter fields and gauge interactions beyond those in the minimal supersymmetric Standard Model [2]. This is certainly the case in models in which the superstring is compactified [7] on some Calabi–Yau manifold [8], and is often true of other compactifications as well. At the time of writing, manifolds with topological properties identical to those of Calabi–Yau manifolds seem [9] to be viable solutions to the string equations of motion. On the other hand, conjectured alternative manifolds [10, 11] whose spin connection is not identified with the gauge connection are not in general solutions to the string equations of motion [12, 13], and have other phenomenological problems [14]. There are orbifold solutions [15] to the string equations of motion which may provide viable frameworks for low-energy phenomenology, but these have not yet been developed. Accordingly, in this paper we concentrate on phenomenological models inspired by Calabi–Yau compactification, although many of the lessons we learn could well be applicable to alternative compactification schemes.

In the case of Calabi–Yau compactifications, we know [7] that the low-energy fields have the quantum numbers of particles in the fundamental **27** representation of E_6, possibly supplemented by a few conjugate pairs of fields from split $\mathbf{27} + \overline{\mathbf{27}}$ representations of E_6. Each **27** (or $\overline{\mathbf{27}}$) representation contains several fields which would mediate proton decay, generate neutrino masses, or yield FCNIs if some of their Yukawa superpotential couplings do not vanish. These include fields with the quantum numbers of minimal supersymmetric Standard Model Higgs doublets H and $\bar{H}$, colour triplet fields D and D^c, and two neutral $SU(3)_c \times SU(2)_L \times U(1)_Y$ invariant fields: ν^c with the quantum numbers of a right-handed neutrino in SO(10), and N, which is an SO(10) singlet. As

for the gauge group, Calabi-Yau compactification, with gauge symmetry broken by the Hosotani [16] mechanism, is fated to yield [17, 18] a four-dimensional gauge group of rank 5 or 6, which therefore contains at least one, and possibly two, additional neutral gauge bosons beyond those in the Standard Model.

The Yukawa superpotential couplings in four dimensions are obtained [19] from the E_8 gauge interactions in ten dimensions. One first projects these onto the E_6-invariant 27^3 (or $\overline{27}^3$) couplings of the four-dimensional zero modes, then decomposes them in terms of representations of the low-energy four-dimensional group. In general, these Yukawa couplings are invariant under the Cartan sub-algebra of E_6. Included among these Yukawa couplings are some which would cause proton decay and/or neutrino masses. The suppression of these unobserved phenomena to acceptably low levels is a non-trivial constraint on superstring compactification schemes. This is one of the issues studied in this paper, and we identify some examples of simple discrete symmetries which would forbid such new interactions.

The Yukawa couplings of the four-dimensional theory are three-index tensors in generation space. This means in particular that there is more than one Higgs H which could *a priori* contribute to the charge $+2/3$ quark mass matrix, and more than one $\bar{H}$ which could contribute to the charge $-1/3$ quark and charge -1 lepton mass matrices. In fact, one can always work in a field basis [20] where only one each of the neutral H and $\bar{H}$ scalar fields has a vacuum expectation value (v.e.v.), and hence contribute to the mass matrices. The other Higgses would still be present in the low-energy spectrum with couplings to quarks and leptons, and could mediate FCNIs [21]. In addition, the tree-level exchanges of scalar D/D^c particles can also give flavour-changing $\bar{q}q\bar{q}q$ or $\bar{q}q\bar{\ell}\ell$ interactions, and loop diagrams can yield additional $\bar{q}q\bar{q}q$, $\bar{q}q\bar{\ell}\ell$ and $\bar{\ell}\ell\bar{\ell}\ell$ interactions. As well as these possible sources of FCNIs, the conventional Z^0 and the additional neutral gauge boson (or bosons) could acquire FCNIs as a result of mixing between conventional charge $-1/3$ quarks and the novel D/D^c fermions. In principle, Calabi-Yau compactifications could yield an extra $SU(2)_N$ or $SU(2)_R$ factor in the low-energy gauge group, with resulting FCNIs mediated by its gauge bosons. In such cases one requires a v.e.v. for a $\tilde{\nu}^c$ field in order to achieve the correct gauge symmetry breaking. We argue below that the generation of a $\tilde{\nu}^c$ v.e.v. is problematic in models based on Calabi-Yau compactifications, and hence we disregard this possibility. Let us also note that Calabi-Yau compactifications were arrived at by demanding that the effective low-energy theory be supersymmetric. So there will also be the FCNI effects from loops involving superpartners of the Standard Model particles, as analysed previously [22] in the case of the supersymmetric Standard Model.

Much of this paper consists of a systematic investigation of the implications of experimental constraints on FCNIs for phenomenological models inspired by the superstring, notably including bounds on the expected Yukawa superpotential couplings. We also look at some other rare processes and precision tests which probe physics beyond the Standard Model. These include CP violation in $K \to \pi\pi$ decay (i.e. ϵ'/ϵ) and the neutron electric dipole moment, $\pi^0 \to e^+e^-$ decay, and the tests of charged-current universality from $\pi \to e\nu$ decay compared with $\pi \to \mu\nu$ decay, and μ decay compared with hadronic charged currents. Our results are collected in the table. Each column

represents a possible class of coupling, and there is one row for each rare process. Each entry in the table gives the corresponding phenomenological bound on the relevant coupling, and the bottom row compiles the best phenomenological bounds for the real and imaginary parts of all the couplings. Some of the bounds are quite severe, although we do not believe that they are fatal to all superstring models. Models in which $\langle 0|\tilde{\nu}^c|0\rangle \neq 0$ have, however, particular difficulties which are avoided if $\langle 0|\tilde{\nu}^c|0\rangle = 0$.

The structure of our paper is as follows. In Section 2 we examine general constraints on low-energy models based on Calabi–Yau compactifications of the heterotic superstring. We mention difficulties inherent in establishing intermediate scales of gauge symmetry breaking. In the absence of such intermediate scales, we argue that a (unique) rank-5 low-energy gauge group is the natural choice. We examine the constraints that nucleon stability imposes on the superpotential couplings of the theory. We show that if one eliminates renormalizable baryon-number-violating couplings from the low-energy theory, then proton stability is assured up to effects of dimension-six operators, suggesting a proton lifetime beyond that accessible to experimental test. We examine the Dirac neutrino mass terms which could occur in the theory. If large tree-level masses are forbidden, there remains the possibility of Dirac neutrino masses induced at the one-loop or two-loop level. We compute the rate for radiative decay of such neutrinos $\nu \rightarrow \nu'\gamma$, which, combined with the cosmological limits on such decays, implies that the neutrinos must be effectively stable. Hence the neutrinos must have masses less than O(100) eV, which is an important constraint on their couplings. The requirement of proton stability already restricts the superpotential terms to two possible combinations. The imposition of naturally vanishing neutrino mass further restricts the possibilities to one of three subcombinations. We show that each of these three possible combinations of superpotential couplings may be simply enforced by possible $\mathbb{Z}_2$ or $\mathbb{Z}_2 \times \mathbb{Z}_2$ symmetries. We also discuss the possible mixing between the familiar charge $-1/3$ down (d) quarks, and the new isosinglet charge $-1/3$ D quarks present in the low-energy theory, which affects the mass matrices and flavour mixings of these particles.

In Section 3 we go through the different rare processes listed in the table caption. In each case we give expressions for the possible contributions due to the novel particles expected in phenomenological models. Then we derive bounds on the flavour-changing couplings assuming plausible values for the $H/\bar{H}$ masses (100 GeV), D/D^c scalar masses (300 GeV) and extra Z' gauge boson mass (300 GeV): it is easy to rescale the bounds by your favourite guesses for these unknown masses. In Section 4 we assess the significance of these phenomenological constraints for superstring models. In particular, we address the following theoretical issues: is it plausible that unwanted Yukawa couplings could be as small as required by the table, or should we ask the compactification process for more zeros? can we tolerate $\langle 0|\tilde{\nu}^c|0\rangle \neq 0$?; and the following experimental issues: which improvements in present limits on rare processes would challenge superstring models most severely? is there a 'best bet' where superstring physics beyond the Standard Model might first appear among rare processes at low energies?

2. SPECIFICATION OF THE LOW-ENERGY MODEL

In this section we develop arguments favouring a unique choice of low-energy gauge group, the number of generations, and well-defined patterns of renormalizable Yukawa couplings which prevent the proton from decaying too rapidly. Some of the discussion follows arguments outlined elsewhere [23, 24]; more arguments are presented in this section and in Section 3.

Our starting point is anomaly-free D = 10 supergravity theory [25] with the gauge group $E_8 \times E_8'$. As is well known, this is also the field theory limit of the $E_8 \times E_8'$ heterotic superstring. We assume a compactification down to four dimensions which preserves one supersymmetry, so that the compact internal space K has SU(3) holonomy, and an SU(3) subgroup of the gauge connection is identified with the spin connection, so that the four-dimensional gauge group is broken: $E_8 \times E_8' \to E_6 \times E_8'$ [7]. Arguments are given elsewhere [12–14] against compactifications in which the gauge and spin connections are not identified, which would yield a d = 4 gauge group of lower rank than E_6, such as SO(10) or SU(5). If K is not simply connected, but has a freely acting discrete symmetry group G: K = $\check{K}$/G, where $\check{K}$ is the covering of K, then E_6 can be broken by non-zero values of Wilson-line integrals winding around the 'holes' in K [16–18]. This leads to one of a number of possible low-energy gauge groups of rank 5 or 6 which include the Standard $SU(3)_c \times SU(2)_L \times U(1)_Y$ Model. This symmetry is in turn spontaneously broken by Higgs v.e.v.'s: $v \equiv \langle 0|H|0\rangle$, $\bar{v} \equiv \langle 0|\bar{H}|0\rangle = O(10^2)$ GeV.

2.1 Intermediate scales?

In the absence of a symmetry breaking scale intermediate between m_W and m_P, many of the possible gauge groups can be excluded by their unsatisfactory predictions [18] for $\sin^2\theta_w$ and the Grand Unification scale m_X. In this section we give three independent arguments disfavouring any such intermediate scale in superstring models, and hence greatly reducing the list of gauge groups to be considered. A further argument against an intermediate scale will be developed in subsequent sections of this paper.

It has been shown [26] that the critical temperature for the phase transition to a vacuum with an intermediate gauge symmetry is very low: $T_c = O(m_W)$. In this case there is a large entropy release $\Delta = (m_I/\tilde{m})^{3/2}$, where m_I is the intermediate scale and $\tilde{m}$ is the scale of supersymmetry breaking. The entropy release Δ would wash out any pre-existing baryon asymmetry unless $m_I \lesssim 10^7$ GeV. This type of argument against an intermediate scale is not completely voided even if the baryon asymmetry is generated at some temperature $O(\tilde{m})$ [27]. Such a low intermediate mass scale is difficult, although not impossible, to reconcile with the experimental value of $\sin^2\theta_w \approx 0.22$, and also runs into problems with baryon decay [27].

Moreover, in no-scale models [28, 29] where the low-mass scales are dynamically determined by dimensional transmutation [29], they are all determined to be $O(10^{0\pm1}) \times m_{\tilde{g}}$ (where $\tilde{g}$ denotes the gluino) with the differences arising only from ratios of coupling constants. In general, the v.e.v.'s of the different neutral fields are intimately linked in such a way that the appearance of one v.e.v. triggers the appearances of others. This is especially true in the model of Ref. [23], where the

supersymmetry-breaking scale $\tilde{m}$ is of order the largest v.e.v. This in turn cannot be much larger than m_W if $\tilde{m}$ is to do its job of protecting the weak gauge hierarchy.

We note also that in the simplest case when there are no light residual components for split $27 + \overline{27}$ supermultiplets, then if one adopts some no-scale or dimensional transmutation scenario as in the previous paragraph, no intermediate scale can be created, as observed in Ref. [18]. Since having such light components requires additional hypotheses about the Wilson-loop expectation values, and is even impossible [17, 18] in some $d = 4$ gauge groups, we are inclined to disregard this possibility.

A further argument against an intermediate scale will subsequently be developed, using the analysis of mass matrices in subsection 2.6. This is preceded by subsections discussing Yukawa couplings of the effective low-energy theory, and phenomenological constraints on them.

2.2 Yukawa couplings: Baryon decay?

The $SU(3)_c \times SU(2)_L \times U(1)_Y$ invariant superpotential couplings contained in the original E_6-invariant 27^3 are:

$$\begin{aligned} W \ni\ & HQu^c + \bar{H}Ll^c + \bar{H}Qd^c \\ & + H\bar{H}N + DD^cN + HL\nu^c + DQQ \\ & + D^cu^cd^c + Dl^cu^c + D^cLQ + D\nu^cd^c \end{aligned} \tag{2.1}$$

The coefficients of the terms in (2.1) must be invariant under the full low-energy gauge group. This requirement imposes no additional constraint if the low-energy gauge group is $SU3)_c \times SU(2)_L \times U(1)^{2 \text{ or } 3}$, but is dangerous if it contains an SU(5) factor, or some possible SU(2) factors. These cases are unacceptable because they force one into theoretical relations between the coefficients in (2.1), which lead to rapid proton decay and/or to unacceptable neutrino masses*). Even if no SU(5) or SU(2) factor is present, to avoid these phenomenological disasters one must impose non-trivial phenomenological constraints on the coefficients of the terms in (2.1), which include all the possible renormalizable baryon-number-violating interactions. To avoid rapid proton decay, one must set to zero the coefficients in *either* the third *or* the fourth row of formula (2.1). Compactification in superstring theories does offer mechanisms which could work these miracles, as has been demonstrated in the case of Calabi–Yau compactification. Some couplings in (2.1) could be forbidden either by discrete symmetries [17] or by topological properties [19] of the manifold of compactification. We will return to this possibility in subsection 2.4.

---

*) The group $SU(2)_R$ could couple together the $\ell^\pm$ and ν mass matrices depending on the physical identification of our fields, whilst $SU(2)_N$ would link the $H\bar{H}N$ mixing term [which must be $O(m_W)$] with the Dirac neutrino mass (which must be much smaller).

One might worry that banning some of the couplings in (2.1) would not be enough by itself to prevent rapid proton decay. The massive modes in superstring models do not mediate proton decay at an observable rate, since their masses are close to the scale of compactification, which is in turn close to the Planck mass. There could be other effective non-renormalizable couplings arising from the E_6 GUT symmetry breaking, and when one integrates out higher string modes. In general, all supersymmetric, Lorentz scalar, higher-dimensional operators invariant under the low-energy gauge group could be generated. If baryon-number-violating operators of dimension five were to arise, they could easily induce proton decay at an observable rate. The Lorentz scalar, supersymmetric, baryon-number-violating operators which one can construct using Standard Model superfields, and are invariant under the $SU(3)_c \times SU(2)_L \times U(1)_Y$ Standard Model gauge group, have been catalogued previously [30]. In the superstring models under discussion there are extra fields in the low-energy theory coming from the other members of the **27** supermultiplet, so new operators may be induced. It is easy to check that the additional baryon-number-violating operators invariant under $SU(3)_c \times SU(2)_L \times U(1)_Y$ which appear are those obtained from similar operators involving Standard Model fields, either by substitution of $\bar{H}$ for L or by substitution of D^c for d^c. So the prospective list of dimension-five baryon-number-violating operators consists of the F-terms: $(QQQL)_F$, $(QQQ\bar{H})_F$, $(e^c u^c u^c d^c)_F$, and $(e^c u^c u^c D^c)_F$. For these terms to be allowed operators they must be invariant under the full low-energy gauge group. In the models under consideration, the gauge group [17, 18] has either rank 5, with a U(1) extension of the Standard Model which is uniquely determined for models arising from Calabi–Yau compactifications, or rank 6 and includes as generators both elements of the Cartan subalgebra of E_6 which are not Standard Model generators. In either case the diagonal U(1) generator of the minimal extension of the gauge group must be a generator of the gauge group of our model (augmented in the rank-6 case by the orthogonal combination in the Cartan subalgebra). If we now check the charge of the prospective F-terms under the minimal extra U(1) required in our models, we find that it is non-zero for each of them. So there are no dimension-five baryon-number-violating operators, involving fields of the **27** supermultiplet, which are invariant under the low-energy gauge group.

If we are willing to consider the possibility of split multiplets, so that some paired elements of $\mathbf{27} + \overline{\mathbf{27}}$ representations survive in the low-energy theory [17], then it is possible to have dimension-five operators which violate baryon number. Indeed, any superpotential F-term which could be contained in

$$W_{eff} \ni \frac{h}{M}\left(\overline{\underline{27}}\,\underline{27}\right)^2 \tag{2.2}$$

[where $M \equiv 2.4 \times 10^{18}$ GeV and h is a coupling which could *a priori* be O(1)] is E_6 invariant, and hence invariant under any low-energy subgroup. This generates baryon-number-violating quartic interactions if one assigns, to particles in the $\overline{\mathbf{27}}$, baryon and lepton numbers that are equal and opposite to those assigned to the corresponding particles in the **27**. However, the operator (2.2) cannot be dressed by renormalizable interactions of the gauge non-singlet fields to give a $d = 6$ operator involving light **27** fields, so this mechanism cannot mediate proton decay. There is,

however, one exceptional case in which (2.2) could be dressed to give a potentially dangerous baryon-number-violating interaction. It has been suggested [7, 10] that in some Calabi–Yau compactifications one might obtain a light gauge singlet field ϕ transforming as a (1, **8**) of $E_6 \times SU(3)$, which couples **27** to $\overline{\mathbf{27}}$ via

$$W \ni h' \phi \underline{27}\,\underline{\overline{27}} \tag{2.3}$$

where the natural order of magnitude of h′ is again O(1). The loop correction depicted in Fig. 1 would then lead to an effective interaction such as

$$\mathcal{L}_{eff} \simeq O\left(\frac{1}{16\pi^2}\right)\frac{h'^2 h}{M m_Q^2} m_\phi (u d e^c u^c) \tag{2.4}$$

where m_Q is the mass of the squark in the $\overline{\mathbf{27}}$, which we have assumed to be larger than that of the slepton in the $\overline{\mathbf{27}}$. If we take h = O(1) and require the coefficient in (2.4) to be less than $(10^{15}\ \text{GeV})^{-2}$, we find that we must require

$$m_\phi \lesssim \left(\frac{m_Q}{10^{14}\,\text{GeV}}\right)^2 \frac{M}{h'^2} \tag{2.5}$$

If h′ = O(1) and $m_Q \sim 10^2$ GeV, this would imply that

$$m_\phi \lesssim 10^{-6}\ \text{GeV} \tag{2.6}$$

which is absurdly small. Of course, it could easily turn out that $h' \lesssim 10^{-5}$ for some reason not yet evident to us, or that $h \ll O(1)$*), or any combination of these. However, it is clear that if light (1, **8**) fields ϕ and light $\overline{\mathbf{27}}$ squarks exist, there is a danger that nucleons would decay too fast thanks to the couplings (2.2) and (2.3), whereas in the absence of light ϕ or $\overline{\mathbf{27}}$ fields the renormalizable couplings (2.1) are the only ones.

In summary: we have seen that we must eliminate some possible superpotential terms in order to avoid dimension-four operators causing proton decay. Having done this, we find there are no dimension-five sources of proton decay in models with low-energy fields from the **27** only. So the experimental observation of proton decay would rule out Calabi–Yau-based superstring models with matter fields in the **27** only, and place stringent demands on models which utilize matter fields from paired pieces of the $\mathbf{27} + \overline{\mathbf{27}}$ as well as the usual fields in the **27**. Finally, we should note that the large unification mass, and absence of dimension-five operators inducing neutron oscillations, implies that there can be no observable neutron oscillations in these theories.

---

*) The analogous suppression appears in the corresponding diagram for baryon decay in conventional supersymmetric GUTs, because one is integrating out a heavy Higgs particle whose couplings to light quarks and leptons are forced to be small.

2.3 Yukawa couplings: Neutrino masses?

The superpotential (2.1) can lead to neutrino masses in two ways. The coupling $HL\nu^c$ can give a Dirac neutrino mass at the tree level, while loop corrections involving the D^cLQ and $D\nu^c\bar{d}^c$ couplings can also generate a Dirac neutrino mass once supersymmetry is broken, if proton decay is eliminated by setting to zero the couplings in the third row of Eq. (2.1) while keeping those in the fourth row. Since the superpotential (2.1) contains no candidate for a Majorana mass term, and since higher-order non-renormalizable superpotential terms cannot generate a large Majorana mass unless there is a large intermediate mass scale (a possibility we discarded in subsection 2.1), we conclude that the Dirac neutrino mass $\lambda_\nu v$ is bounded by the cosmological bound [31] $m_\nu \lesssim 25$ eV, in which case $\lambda_\nu \lesssim O(10^{-9})$. It is therefore very tempting to set $\lambda_\nu = 0$, possibly invoking a discrete symmetry and/or a topological zero as already mentioned in connection with proton decay. Candidate discrete symmetries will be mentioned in subsection 2.4.

Even if $\lambda_\nu = 0$, the one-loop diagrams of Figs. 2a and 2b will induce a radiative Dirac neutrino mass*). Working in a basis where the d($\tilde{d}$) and D ($\tilde{D}$) mass matrices m_α (μ_β) are diagonal in flavour space, and denoting the $\nu^{ci}d^{c\alpha}D^\beta$ ($L^iQ^\alpha D^{c\beta}$) couplings by $(\lambda_{10})_{i\alpha\beta}$ ($(\lambda_9)_{i\alpha\beta}$), we find that

$$\text{fig.2a} \Rightarrow M^a_{ij}(\nu) = \sum_{\alpha,\beta} A_D (\lambda_{10})_{i\alpha\beta}(\lambda_9)_{j\alpha\beta} m_\alpha m_\beta I^a(\tilde{D}_\beta, \tilde{D}^c_\beta) \tag{2.7a}$$

$$\text{fig.2b} \Rightarrow M^b_{ij}(\nu) = \sum_{\alpha,\beta} A_d (\lambda_{10})_{i\alpha\beta}(\lambda_9)_{j\alpha\beta} m_\alpha m_\beta I^b(\tilde{d}_\alpha, \tilde{D}_\beta) \tag{2.7b}$$

In expressions (2.7), A_D and A_d are the trilinear soft supersymmetry-breaking coefficients for the $\tilde{D}\tilde{D}^cN$ and $\tilde{d}\tilde{d}^c\bar{H}$ effective scalar couplings respectively, and

$$I^a(1,2) = \frac{1}{16\pi^2}\frac{1}{m_2^2 - m_1^2}\ln\frac{m_2^2}{m_1^2} \to \frac{1}{16\pi^2}\frac{1}{m_1^2} \tag{2.8a}$$

$$I^b(1,2) = \frac{1}{16\pi^2}\left(\frac{1}{m_2^2 - m_1^2}\right)^2\left[m_2^2 \ln\frac{m_2^2}{m_1^2} - (m_2^2 - m_1^2)\right] \to \frac{1}{32\pi^2}\frac{1}{m_1^2} \tag{2.8b}$$

where the limits for $m_2^2 \to m_1^2$ have been exhibited explicitly. We evaluate $m(\nu)$ [formulae (2.7) and (2.8)] by taking $m_D \approx$ a typical supersymmetry-breaking scale $m_{1/2}$ [see Eq. (2.9)] and the soft supersymmetry-breaking squark masses squared to be

$$m^2_{\tilde{d}} \sim m^2_{\tilde{d}^c} \sim m^2_{\tilde{D}} \sim m^2_{\tilde{D}^c}$$

$$= -\frac{2}{3\pi^2}\int_{\ln m_X}^{\ln m_W} dt\, g_3^2 m_{\tilde{g}}^2 \approx \frac{8}{3\pi}\alpha_3 m_{1/2}^2 \ln(m_X/m_W) \simeq 3m_{1/2}^2 \tag{2.9}$$

---

*) One-loop neutrino mass generation is also considered in Ref. [32], with reference to experimental indications of neutrino mass [33], and the possibility of the Mikheyev-Smirnov effect [34].

in which case

$$16\pi^2 I^a \approx 0.25/m_{1/2}^2 \quad , \quad 16\pi^2 I^b \approx 0.23/m_{1/2}^2 \tag{2.10}$$

so that, since $A_D \approx A_d$ in first approximation,

$$m_\nu = M^a(\nu) + M^b(\nu) \simeq \frac{A_D \lambda_9 \lambda_{10} m_b}{32\pi^2} \tag{2.11}$$

where only the heaviest charge $-1/3$ quark contribution has been retained. To get m_ν [Eq. (2.11)] less than 25 eV so as to avoid an overdense Universe, we find for a typical value of $A_d = O(1)$ that

$$\lambda_9 \lambda_{10} \lesssim 10^{-6} \tag{2.12}$$

must be imposed. This constraint is shown as the (23,7) and (23,8/9/10) entries in the table.

If the D^cQL superpotential coupling is absent, we can still induce a Dirac neutrino mass at the two-loop level via the Du^ce^c and $Dd^c\nu^c$ couplings, once supersymmetry is broken (Figs. 2c and 2d). This gives a Dirac neutrino mass that we may roughly estimate to be

$$m_\nu \sim \frac{\lambda_8 \lambda_{10} \lambda_2 \lambda_1 A A_D}{(16\pi^2)^2} m_b \tag{2.13}$$

where A denotes A_d or A_H. For this not to exceed the cosmological limit $m_\nu \lesssim O(25\text{ eV})$ for typical values $A_D \simeq 1 \simeq A_d$, we should therefore require that

$$\lambda_8 \lambda_{10} \lambda_2 \lambda_1 \lesssim 10^{-4} \tag{2.14}$$

which is clearly less stringent than the previous constraint.

In order to ensure the validity of these bounds we must verify that our neutrinos really are constrained by cosmology. From the analysis of Sarkar and Cooper [31] we know that the combination of particle and astrophysical constraints requires the neutrinos to have mass less than the effective threshold in $\nu \to \nu' e^+ e^-$ decay, i.e. $m_\nu < O(1\text{ MeV})$. Then the primary decay mode of the heavy neutrinos would be $\nu \to \nu'\gamma$ via the diagrams of Fig. 3, for the case where the neutrino mass arose as a one-loop effect. One may roughly estimate the lifetime*) for this decay as

$$\tau_\nu = \Gamma_\nu^{-1} \quad ; \quad \Gamma_\nu = \frac{\alpha}{4} a_\nu^2 m_\nu \tag{2.15a}$$

---

*) The lifetime for $\nu' \to \nu\gamma$ in these theories is computed in more detail in Ref. [35], which also discusses astrophysical constraints on this decay.

where

$$a_\nu \sim \frac{\lambda_9 \lambda_{10}}{16\pi^2}\left(\frac{m_\nu m_d}{m_{\tilde{D}}^2}\right) \tag{2.15b}$$

which must be compared with the astrophysical limits for neutrinos decaying via this mode:

$$\tau_\nu \lesssim 2\times 10^8 \text{ s} \cdot \left(m_\nu/1\text{MeV}\right)^{-2} \tag{2.16}$$

These are in contradiction for neutrinos in the range below 1 MeV which we are considering. Hence these neutrinos must be effectively cosmologically stable, and thus satisfy the cosmological bound $m_\nu \lesssim$ O(25 eV). For neutrinos where mass and decay originate in two-loop processes we expect the decay to proceed even more slowly. Also in this case it would require $\lambda_1\lambda_2\lambda_8\lambda_{10} > 10^{-4}$ (i.e. $\lambda > 0.1$) in order to get neutrinos above the mass limit for cosmically stable neutrinos, which seems unlikely.

So we see that neutrino masses, if banished at the tree level, may still arise at the one- or two-loop level, and that the cosmological constraint on effectively stable neutrinos then gives sharp restrictions on the magnitude of the superpotential couplings allowed. We wish to emphasize that the absence of Majorana mass terms for the theory implies that only lepton-number-conserving Dirac neutrino masses may be present, and that the massive neutrinos would be Dirac fermions. In particular, whilst this opens up the possibility of observing neutrino flavour oscillations, or direct mass determination, lepton-number-violating processes such as neutrinoless double beta decay or neutrino–antineutrino oscillations remain forbidden. The experimental observation of such lepton-number-violating processes would effectively rule out this class of superstring models. Finally, we note that in the next section examples will be given of simple discrete symmetries which would naturally enforce the masslessness of neutrinos.

2.4 Discrete symmetries?

It was commented earlier that the desired pattern of Yukawa couplings could be imposed by postulating certain discrete symmetries or invoking topological zeros. We would now like to present examples of discrete symmetries which would ensure proton stability and forbid neutrino masses. The first three terms in formula (2.1) give conventional charged lepton and quark masses, and are therefore essential, as are the next two, which provide $H\bar{H}$ mixing and D masses, respectively. We call these first five terms collectively W_0. We saw in subsection 2.2 that *either* the third *or* the fourth row of (2.1) should vanish. We saw in subsection 2.3 that to forbid a Dirac neutrino mass we should forbid the $HL\nu^c$ coupling in (2.1), and also *either* the D^cLQ and $D\ell^cu^c$ *or* the $D\nu^cd^c$ coupling, so as to avoid the radiative masses (2.11) and (2.13). Therefore the allowable superpotentials are

$$W_1 \equiv W_0 + Dd^c\nu^c \tag{2.17a}$$

$$W_2 \equiv W_0 + D^cQL + Du^ce^c \tag{2.17b}$$

$$W_3 \equiv W_0 + DQQ + D^cu^cd^c \tag{2.17c}$$

The first of these can be selected by the following Z_2 extension of conventional R-parity:

$$R_1 = \begin{cases} -1 & \text{for } Q, u^c, d^c, L, e^c, D, D^c \\ +1 & \text{for } H, \bar{H}, \nu^c, N \end{cases} \tag{2.18a}$$

i.e. $R_1 = (-1)^{3B+L-2S}$: B(D) = +1/3, B(D^c) = −1/3, B, L(ν^c) = 0, B, L(N) = 0. The second option (2.17b) can be selected by the $Z_2 \times Z_2'$ discrete symmetry,

$$\begin{aligned} Z_2 &: \quad (3, \bar{3})|_{SU(3)} \to (-1) \times (3, \bar{3})|_{SU(3)} \\ Z_2' &: \quad \nu^c \to (-1) \times \nu^c \end{aligned} \tag{2.18b}$$

whilst the third option (2.17c) can be selected by the alternative $Z_2 \times Z_2'$ discrete symmetry,

$$\begin{aligned} Z_2 &: \quad (L, e^c, \nu^c) \to (-1) \times (L, e^c, \nu^c) \\ Z_2' &: \quad \nu^c \to (-1) \times \nu^c \end{aligned} \tag{2.18c}$$

We have found no generation-independent discrete symmetry which allows the radiative mass terms (2.11) and (2.13) but not the tree-level mass term $HL\nu^c$. Since any discrete symmetry of the type (2.18) is conserved by conventional supersymmetry-breaking terms, and since the scalar fields H, $\bar{H}$, and N which we believe have v.e.v.'s are all inert, this observation is completely natural. Notice also that because H, $\bar{H}$, and N are inert under the discrete symmetries (2.18), none of these poses a domain wall problem [36].

The options (2.17) characterize the ambiguity we find in the superstring Yukawa couplings. In the next section we will use various rare processes to bound the allowed coefficients, which we denote by

$$\begin{aligned} W = {} & \lambda_2 \bar{H} L L^c + \lambda_3 \bar{H} Q d^c + \lambda_1 H Q u^c \\ & + \lambda_4 H \bar{H} N + \lambda_5 D D^c N \\ & + \lambda_6 D Q Q + \lambda_7 D^c u^c d^c \\ & + \lambda_8 D L^c u^c + \lambda_9 D^c L Q + \lambda_{10} D \nu^c d^c \end{aligned} \tag{2.19}$$

The significance of these bounds will be discussed in Section 4.

2.5 Low-energy gauge group: rank 5?

We will now discuss the four-dimensional gauge group, and give some reasons why the minimal rank-5 choice $SU(3)_c \times SU(2)_L \times U(1)_Y \times U(1)_E$ is preferred [24]. The $H\bar{H}N$ and DD^cN Yukawa couplings in (2.1) can easily [23] drive $m_N^2 < 0$ and generate the phenomenologically necessary v.e.v. $\langle 0|N|0\rangle \equiv x \neq 0$. Therefore the initial value of the rank of the d = 4 gauge group could well be one

more than the Standard Model value of 4, namely rank 5. However, we will now argue that the Yukawa couplings needed to drive $m^2_{\tilde{\nu}^c} < 0$ and hence generate $\langle 0|\tilde{\nu}^c|0\rangle \equiv y = O(1)$ TeV are either absent or are constrained by our subsequent phenomenological analysis to be too small to be useful. Therefore, one cannot reduce the d = 4 rank by more than one, and it is not possible to make a dynamical model based on rank 6. In the arguments leading to this conclusion we will assume there are no arbitrary generation-dependent zeros in the Yukawa couplings of (2.1). Some of our arguments could be avoided by postulating convenient generation-dependent zeros therein. Such zeros appear and play a crucial role in the rank-6 models of Ref. [37], which employ an intermediate scale of the type argued against in subsection 2.1.

We first argue that the appropriate criterion for getting $y = \langle 0|\tilde{\nu}^c|0\rangle \neq 0$ is indeed to be able to drive $m^2_{\tilde{\nu}^c} < 0$. The first term in a Taylor series expansion of the effective scalar potential around $\tilde{\nu}^c = 0$, which could in principle destabilize the origin, is one linear in $\tilde{\nu}^c$. However, we recall from the superpotential (2.1) that ν^c only appears in the $HL\nu^c$ and $Dd^c\nu^c$ couplings. Recalling that we expect $\langle 0|\tilde{\nu}|0\rangle = \langle 0|\tilde{D}|0\rangle = \langle 0|\tilde{d}^c|0\rangle = 0$, we see that no linear term in $\tilde{\nu}^c$ can arise. Hence we look at the quadratic term $m^2_{\tilde{\nu}^c}|\tilde{\nu}^c|^2$.

One or the other of the Yukawa couplings $HL\nu^c$, $Dd^c\nu^c$ would be necessary to drive $m^2_{\tilde{\nu}^c} < 0$ via the renormalization group. To rule this out, we need to distinguish the two distinct possibilities for the superpotential which solve the baryon decay problem: *either* the fourth line of (2.1) vanishes, *or* the third line vanishes. In the first case there is no $Dd^c\nu^c$ coupling, only the $HL\nu^c$ coupling which must be very small ($\lesssim 10^{-9}$) so as to get an acceptably light neutrino, and hence cannot drive $m^2_{\tilde{\nu}^c} < 0$. Indeed, the natural possibility (2.17c) suggested by the search for plausible discrete symmetries is that in this case the ν^c has no Yukawa couplings at all. If, on the other hand, the third line of (2.1) vanishes, then the search for plausible discrete symmetries in the previous subsection reveals two possibilities: (2.17b) in which there is again no Yukawa coupling of the ν^c, and (2.17a) in which the $Dd^c\nu^c$ coupling appears. Thus the unique possibility consistent with plausible discrete symmetries is that $Dd^c\nu^c$ drives $m^2_{\tilde{\nu}^c} < 0$. Even if one does not invoke such a discrete symmetry, we know on phenomenological grounds that the $HL\nu^c$ coupling must be too small to be useful.

To finally dispose of the possibility that $\langle 0|\tilde{\nu}^c|0\rangle \neq 0$, we need to establish that the $Dd^c\nu^c$ coupling λ_{10} cannot drive $m^2_{\tilde{\nu}^c} < 0$, which entails arguing that the coupling cannot be very large. The argument for this proceeds in two steps. In subsection 2.6 we analyse the mass matrix for the d and D (d^c and D^c) quarks, which arises if $y \equiv \langle 0|\tilde{\nu}^c|0\rangle \neq 0$, and argue that $y \lesssim O(10)(\langle 0|N|0\rangle \equiv x)$, while $x = O(1)$ TeV. This means that the mixing between d-quarks and D-quarks cannot be arbitrarily small. The resulting flavour-changing neutral-current effects are analysed in Section 3, where it is argued that K^0–$\bar{K}^0$ mixing and $K_L \to \mu^+\mu^-$ restrict $\lambda_{10} \lesssim O(10^{-2})$, which is too small to generate $y = \langle 0|\tilde{\nu}^c|0\rangle \neq 0$. On the other hand, no disastrous neutral-current effects will arise if $y = \langle 0|\tilde{\nu}^c|0\rangle = 0$, so favouring a rank-5 group in four dimensions.

2.6 d/D mixing?

We consider here the mass matrix mixing d/D and d^c/D^c which is provided by the superpotential (2.19) in the general case that $\bar{v} \equiv \langle 0|\bar{H}|0\rangle$, $x \equiv \langle 0|N|0\rangle$, and $y \equiv \langle 0|\tilde{\nu}^c|0\rangle \neq 0$. For simplicity and to

illustrate the general principles we consider the case of one flavour each of d, D, d^c, and D^c. The mass matrix M is given by

$$(d^c, D^c)\begin{pmatrix} \lambda_3\bar{v} & \lambda_{10}y \\ 0 & \lambda_5 x \end{pmatrix}\begin{pmatrix} d \\ D \end{pmatrix} + h.c. \tag{2.20}$$

and can be diagonalized by a biunitary transformation:

$$M_{diag} = V_R M V_L^\dagger \tag{2.21}$$

In our case the $V_{L,R}$ are 2×2; in general they are $2N_g \times 2N_g$ (i.e. probably 6×6) unitary matrices. In our case

$$V_{R,L} = \begin{pmatrix} \cos\theta_{R,L} & \sin\theta_{R,L} \\ -\sin\theta_{R,L} & \cos\theta_{R,L} \end{pmatrix} \tag{2.22}$$

and in the limit which is likely to be of interest to us, where $\lambda_3\bar{v} \ll (\lambda_5^2x^2 + \lambda_{10}^2y^2)^{1/2}$ and $m_{Z'}^2 \gg m_Z^2$, we have

$$\theta_L \approx \frac{\lambda_3\lambda_{10}\bar{v}y}{(\lambda_5^2x^2 + \lambda_{10}^2y^2)} \tag{2.23a}$$

$$\tan\theta_R \approx -\frac{\lambda_{10}y}{\lambda_5 x} \tag{2.23b}$$

while the mass eigenvalues are

$$m_d^{phys} \approx \frac{\lambda_3\bar{v}\,\lambda_5 x}{(\lambda_5^2x^2 + \lambda_{10}^2y^2)^{1/2}} \tag{2.24a}$$

$$m_D^{phys} \approx (\lambda_{10}^2y^2 + \lambda_5^2x^2)^{1/2} \tag{2.24b}$$

We now discuss some phenomenological implications of the results (2.23) and (2.24).

It is clear from (2.24a) that the physical value of m_d is greatly reduced if $\lambda_{10}y \gg \lambda_5 x$. Since charged leptons also get their masses from $\langle 0|\bar{H}|0\rangle \equiv \bar{v}$, a fair measure of this potential suppression is

to compare m_e with m_d, m_μ with m_s, and m_τ with m_b. (Another possible comparison would be m_u with m_d, etc., but the interpretation of this would be clouded by the unknown ratio of $\langle 0|H|0\rangle \equiv v/\bar{v}$.) Since $m_d > m_e$, $m_s > m_\mu$, and $m_b > m_\tau$, there is no evidence that $x \ll y$, and we infer conservatively that

$$y \lesssim O(10)x \tag{2.25}$$

This immediately means that the D-'quarks' (2.24b) cannot be very heavy, since $H\bar{H}$ mixing already requires $x = O(1)$ TeV. Hence D-'quarks' are accessible to phenomenological analyses of flavour-changing neutral interactions and other rare processes, as discussed in Section 3. The result (2.25) also means that the mixing angle θ_R (2.23b) cannot be very close to $\pi/2$. Since the d^c and D^c have identical $SU(3)_c \times SU(2)_L \times U(1)_Y$ quantum numbers, this mixing has no effect on Standard Model couplings. However, models with rank ≥ 5 have a second U(1) gauge boson Z′ with mass O(x) whose couplings to the d^c and D^c are in general different. This means that the Z′ couplings to d_R-, s_R-, and b_R-quarks contain in general flavour-changing pieces or order

$$\epsilon_R^2 \sim \frac{\lambda_5^2 x^2}{\lambda_{10}^2 y^2} \quad (\lambda_5 x \ll \lambda_{10} y) \qquad \text{or} \qquad \frac{\lambda_{10}^2 y^2}{\lambda_5^2 x^2} \quad (\lambda_{10} y \ll \lambda_5 x) \tag{2.26}$$

The left-handed mixing angle θ_L (2.23a) could be somewhat smaller, but since the d and D have different $SU(2)_L \times U(1)_Y$ couplings, it means that the Z couplings to d_L-, s_L-, and b_L-quarks contain in general flavour-changing pieces of order

$$\epsilon_L^2 \sim \theta_L^2 \sim \frac{\lambda_3^2 \bar{v}^2 \lambda_{10}^2 y^2}{(\lambda_5^2 x^2 + \lambda_{10}^2 y^2)^2} \tag{2.27}$$

Since we know m_Z, but not $m_{Z'}$, there are more severe bounds on flavour-changing couplings of the Z (2.27) than on those of the Z′ (2.26). However, these bounds are in general of comparable magnitude, as discussed in subsections 3.1.1, 3.1.2, etc. These bounds lead to the conclusion that $\lambda_{10} \lesssim O(10^{-2})$, which suggests that the $Dd^c\nu^c$ coupling is not large enough to generate $\langle 0|\tilde{\nu}^c|0\rangle \neq 0$. The mixing (2.23a) also leads in principle to an apparent violation of unitarity in the Kobayashi–Maskawa matrix, as discussed in subsection 3.6.3, but experiment does not provide important constraints on this effect.

3. PHENOMENOLOGICAL BOUNDS ON RARE PROCESSES IN SUPERSTRING MODELS

We now develop the results shown in the table. Our calculations are divided into subsections dealing with K physics, D physics, B physics, μ physics, CP violation, and weak universality tests.

3.1 K physics

3.1.1 K^0-$\bar{K}^0$ mixing

This is well described by the classic charm loop calculation [38] which yields an effective interaction

$$\mathcal{L}_{eff} = \frac{G_F}{\sqrt{2}} \frac{\alpha}{4\pi} \frac{m_c^2}{m_W^2 \sin^2\theta_W} \sin^2\theta_c \cos^2\theta_c \left[\bar{s}_L \gamma_\mu d_L\right]^2 \tag{3.1}$$

with its matrix element between K^0 and $\bar{K}^0$ approximated by vacuum saturation. This approximation is not yet known to be wrong, so we adopt it hereafter and therefore demand that any $(\bar{s}_L\gamma^\mu d_L)^2$ or $(\bar{s}_R\gamma^\mu d_R)^2$ operator generated by physics beyond the Standard Model should have a coefficient C_{LL} or C_{RR} of magnitude smaller than that in (3.1):

$$|C_{LL}|, |C_{RR}| \lesssim \frac{G_F}{\sqrt{2}} \frac{\alpha}{4\pi} \frac{m_c^2}{m_W^2 \sin^2\theta_W} \sin^2\theta_c \cos^2\theta_c \approx 0.5 \times 10^{-12}\ \text{GeV}^{-2} \tag{3.2}$$

For future reference in the CP violation subsection 3.1.5, we note here [39] that the experimental constraint

$$|\mathrm{Im}\, M_{K\bar{K}}| \simeq 1.5 \times 10^{-3} |\mathrm{Re}\, M_{K\bar{K}}| \tag{3.3}$$

imposes the following constraint on the imaginary parts of C_{LL} and C_{RR}:

$$|\mathrm{Im}\, C_{LL}|, |\mathrm{Im}\, C_{RR}| \lesssim 0.8 \times 10^{-15}\ \text{GeV}^{-2} \tag{3.4}$$

New physics often generates an $(\bar{s}_L\gamma^\mu d_L)\,(\bar{s}_R\gamma_\mu d_R)$ operator, which is estimated [40] to have a matrix element about eight times larger than that of the $(\bar{s}_L\gamma^\mu d_L)^2$ operator. Therefore its coefficient C_{LR} should be at least a factor of 8 smaller than C_{LL}:

$$|C_{LR}| \lesssim 0.6 \times 10^{-13}\ \text{GeV}^{-2}, \quad |\mathrm{Im}\, C_{LR}| \lesssim 1.2 \times 10^{-16}\ \text{GeV}^{-2} \tag{3.5}$$

We now use Eqs. (3.2) and (3.5) to constrain superstring contributions to the real part of the K^0-$\bar{K}^0$ mass mixing matrix: the results (3.4) and (3.5) for the imaginary parts will be used in subsection 3.1.5.

The neutral Higgs exchange diagram of Fig. 4a gives

$$\mathcal{L}_{eff} = \frac{\lambda_3^2}{m_H^2} (\bar{s}_R d_L)(\bar{s}_L d_R) = \frac{\lambda_3^2}{2m_H^2} (\bar{s}_R \gamma^\mu d_R)(\bar{s}_L \gamma_\mu d_L) \tag{3.6}$$

Using (3.5) we conclude that

$$\frac{\lambda_3^2}{m_{\bar{H}}^2} \lesssim 1.2 \times 10^{-13}\ \mathrm{GeV}^{-2} \tag{3.7}$$

yielding the (1,3) entry in the table.

Next we turn to the Z and Z′ exchange diagrams of Fig. 4b. If $y \equiv \langle 0|\bar{\nu}|0\rangle \neq 0$, then, as discussed in subsection 2.6, the $Dd^c\nu^c$ vertex in the superpotential (2.1) makes a contribution to the (d, D) mass matrix, which means that the physical d_L is actually a mixture of SU(2) doublet and singlet states:

$$d_L^{\text{phys}} = d_L + \epsilon_L D : \quad \epsilon_L = O\left(\frac{\lambda_3 \bar{\nu}\, \lambda_{10} y}{\lambda_{10}^2 y^2 + \lambda_5^2 x^2}\right) \tag{3.8}$$

where $x \equiv \langle 0|N|0\rangle$ and we have assumed that $\bar{\nu} \ll x, y$. In the absence of any good reason to believe that this is diagonal in generation, we conclude that a flavour-changing Z^0 vertex of the form

$$O(\epsilon_L^2)\sqrt{g_2^2+g'^2}\left(\bar{s}_L^{\text{phys}} \gamma^\mu d_L^{\text{phys}}\right) Z^0_\mu \tag{3.9}$$

will usually be generated. There is no corresponding off-diagonal coupling of the Z^0 to the s_R and d_R, since the d^c and D^c fields have identical $SU(2)_L \times U(1)_Y$ quantum numbers. Since the Z′ has in general different U(1)′ charges for the d^c and D^c, the Z′ will have flavour-changing vertices of the form

$$O(\epsilon_R^2)\, g'\left(\bar{s}_R^{\text{phys}} \gamma^\mu d_R^{\text{phys}}\right) Z'_\mu \tag{3.9′}$$

where

$$d_R^{\text{phys}} = d_R + \epsilon_R D_R : \quad \epsilon_R = O\left(\frac{\lambda_{10} y}{\lambda_6 x}\right) \tag{3.8′a}$$

if $\lambda_{10} y \ll \lambda_6 x$, and

$$d_R^{\text{phys}} = D_R + \epsilon_R d_R : \quad \epsilon_R = O\left(\frac{\lambda_6 x}{\lambda_{10} y}\right) \tag{3.8′b}$$

if $\lambda_{10} y \gg \lambda_6 x$. Using Eqs. (3.2) and (3.9), we get the bound

$$\frac{\epsilon_L^4}{m_Z^2}\left(g_2^2 + g'^2\right) < 0.5 \times 10^{-12}\ \mathrm{GeV}^{-2} \tag{3.10}$$

which yields the (1,9) entry in the table. Using Eqs. (3.2) and (3.9′), we infer

$$\frac{\epsilon_R^4}{m_{Z'}^2}\, g'^2 < 0.5\times10^{-12}\ \mathrm{GeV}^{-2} \tag{3.10′}$$

which yields limits similar to those given by (3.10) for Z′ boson masses in a plausible [23] range of several hundred GeV, and shown in the (1,10) entry in the table.

Next we turn to the loop diagrams of Figs. 4c to 4e. Figures 4c and 4d with only D and $\widetilde{D}$ exchanges give

$$\mathcal{L}_{eff} \sim \text{either}\ \frac{\lambda_6^4}{64\pi^2}\frac{1}{2m_D^2}\left(\bar{s}_L\gamma^\mu d_L\right)^2 \ \text{or}\ \frac{\lambda_{10}^4}{64\pi^2}\frac{1}{2m_D^2}\left(\bar{s}_R\gamma^\mu d_R\right)^2 \tag{3.11}$$

whilst the corresponding diagrams with D^c and $\widetilde{D}^c$ exchanges give

$$\mathcal{L}_{eff} \sim \text{either}\ \frac{\lambda_7^4}{64\pi^2}\frac{1}{2m_{D^c}^2}\left(\bar{s}_R\gamma^\mu d_R\right)^2 \ \text{or}\ \frac{\lambda_8^4}{64\pi^2}\frac{1}{2m_{D^c}^2}\left(\bar{s}_L\gamma^\mu d_L\right)^2 \tag{3.12}$$

in cases (2.17b) *or* (2.17c) respectively. Figure 4e with D/D^c mixing gives

$$\mathcal{L}_{eff} \sim \left(\text{either}\ \frac{\lambda_6^2\lambda_7^2}{64\pi^2}\frac{m_{DD^c}^2}{2m_D^2 m_{D^c}^2} \ \text{or}\ \frac{\lambda_8^2\lambda_{10}^2}{64\pi^2}\frac{m_{DD^c}^2}{2m_D^2 m_{D^c}^2}\right)\times\left(\bar{s}_R\gamma^\mu d_R\right)\left(\bar{s}_L\gamma_\mu d_L\right) \tag{3.13}$$

Imposing the constraint (3.2) on the coefficients in (3.11) yields the (1,4) and (1,8) entries in the table, whilst (3.12) yields the (1,5) and (1,6) entries. The magnitude of the D/D^c mixing term $m_{DD^c}^2$ in (3.13) depends on an unknown supersymmetry-breaking scale factor as well as $\lambda_5 x$. Imposing the constraint (3.5) on the coefficients in (3.13) could give slightly tighter constraints on the products $\lambda_6\lambda_7$ and $\lambda_8\lambda_{10}$ if the mixing were maximal, but their interpretation would be less direct, and we have chosen to omit them from the table.

This concludes our analysis of K^0–$\overline{K}^0$ mixing, which will be mirrored in subsections 3.2.1 and 3.3.1 on D^0–$\overline{D}^0$ and B^0–$\overline{B}^0$ mixing, respectively.

3.1.2 $K_L \to \mu\mu$

The mechanisms under consideration can give short-distance contributions to $K_L \to \mu\mu$ decay while we bound [38] as follows:

$$\frac{\Gamma_{sd}(K_L \to \mu\mu)}{\Gamma(K^+ \to \mu^+\nu)} = \frac{\Gamma(K_L \to \text{all})}{\Gamma(K^+ \to \text{all})} \frac{B_{sd}(K_L \to \mu\mu)}{B(K^+ \to \mu^+\nu)} \tag{3.14}$$

Using $\Gamma(K_L \to \text{all}) = 0.19 \times 10^8\ s^{-1}$, $\Gamma(K^+ \to \text{all}) = 0.8 \times 10^8\ s^{-1}$, and assuming $B_{sd}(K_L \to \mu\mu) = (1 \text{ to } 5) \times B_{obs}(K_L \to \mu\mu) = (1 \text{ to } 5) \times 10^{-8}$, Eq. (3.14) yields

$$\frac{\Gamma_{sd}(K_L \to \mu\mu)}{\Gamma(K^+ \to \mu^+\nu)} \lesssim 2 \times 10^{-8} \tag{3.15}$$

The effective interaction generating $K^+ \to \mu^+\nu$ decay in the Standard Model is

$$\mathcal{L}_{eff} = \frac{4G_F \sin\theta_C}{\sqrt{2}} (\bar{\mu}_L \gamma^\alpha \nu_L)(\bar{s}_L \gamma_\alpha d_L) \tag{3.16}$$

Therefore the bound (3.15) tells us that an effective interaction

$$\mathcal{L}_{eff} = C_0 O \tag{3.17}$$

contributing to $K_L \to \mu\mu$ decay must have a coefficient C_0 obeying

$$|C_0| < 1 \times 10^{-9} R^{-1}\ \text{GeV}^{-2} \tag{3.18}$$

where

$$R \equiv \frac{\langle \mu\mu | O | K_L \rangle}{\langle \mu^+\nu | (\bar{\mu}_L \gamma^\alpha \nu_L)(\bar{s}_L \gamma_\alpha d_L) | K^+ \rangle} \tag{3.19}$$

The bound (3.18) will now be used to constrain superstring contributions to $K_L \to \mu\mu$.

The neutral Higgs diagram of Fig. 5a gives

$$\mathcal{L}_{eff} = \frac{\lambda_2 \lambda_3}{m_H^2} (\bar{s}_R d_L)(\bar{\mu}_L \mu_R) \tag{3.20}$$

for which

$$R = \frac{m_K^2}{m_\mu m_s} \simeq 15 \tag{3.21}$$

Inserting (3.21) into the bound (3.18) we deduce the bound

$$\frac{\lambda_2 \lambda_3}{m_H^2} \lesssim 0.7 \times 10^{-10}\ \text{GeV}^{-2} \tag{3.22}$$

yielding the result spread across entries (2,2) and (2,3) of the table. In the case of Fig. 5b, the discussion of D_L/d_L mixing in subsection 3.1.1 tells us that Z^0 exchange contributes

$$\mathcal{L}_{eff} \simeq \frac{g_2^2+g'^2}{2m_Z^2}\epsilon_L^2(\bar{\mu}\gamma^\mu\frac{\gamma_5}{2}\mu)(\bar{s}_L\gamma_\mu d_L) \tag{3.23}$$

with ϵ_L given by (3.8), where we have exploited the near-absence of the Z^0 vector coupling to $\mu^\pm$. For the operator in (3.22), R = 1 so that the bound (3.18) provides us with

$$\frac{g_2^2+g'^2}{m_Z^2}\epsilon_L^2 < 2\times10^{-9} \tag{3.24}$$

which yields the (2,9) entry in the table.

As for Z′ exchange, D_R/d_R mixing, which is larger than D_L/d_L mixing, can also contribute to $K_L \to \mu^+\mu^-$. The bound corresponding to (3.24) is

$$\frac{g'^2}{m_Z^2}\epsilon_R^2 < 2\times10^{-9} \tag{3.24′}$$

with ϵ_R given by Eq. (3.8′), which leads to the bound shown in the (2,10) entry in the table.

The loop diagrams of Fig. 5c (together with the appropriate set of self-energy contributions and counter terms) can be evaluated by first determining the effective $\bar{f}_L\gamma_\mu f_L V^\mu$ (V = γ, Z, Z′) vertices using the Gaillard and Lee (GL) methods of Ref. [38] that make use of the Ward identities

$$q_\mu\Gamma_V^\mu = m_V\Gamma_{\phi_V} \tag{3.25}$$

where for $m_V \neq 0$, Φ_V is the scalar eaten by V, and Γ_X is the generic full effective $X\bar{f}f'$ vertex for on-shell fermions and an off-shell boson X of momentum transfer q. Since γ-exchange does not contribute to $K \to \mu\mu$ (nor to the decay $K \to \pi\bar{\nu}\nu$ to be considered in the next subsection), discussion of the $\gamma\bar{f}f'$ vertex is deferred to subsection 3.1.4. For the effective $Z\bar{f}f'$ vertex, the result should be numerically similar to the GL result with the replacements $\sin\theta_C g^2/2m_W^2 \to \lambda_j^2/m_D^2$ and $m_c^2 \to m_i^2$, where m_i is the mass of the internal fermion, giving an effective four-fermion interaction of the form:

$$\mathcal{L}_{eff} \simeq \frac{\lambda_i^2}{m_D^2}\frac{m_i^2 G_F}{4\pi^2\sqrt{2}}\ln(m_D^2/m^2)(\bar{f}_L\gamma^\mu f'_L)\left[\bar{l}\gamma^\mu\frac{\gamma_5}{2}l + \bar{\nu}_L\gamma^\mu\nu_L\right] \tag{3.26}$$

where m is the largest of the m_i and the external masses. Taking $\bar{f}f = \bar{s}d$, a vertex $\propto \lambda_{9,10}^2$ would correspond to $m_i = m_\nu$, so no useful limit is obtained. In the case of $\lambda_{6,7}$ the only useful limits are for the case where the t-quark is exchanged. Since R = 1 for the operators (3.26), we find

$$\lambda_{6,7}(t) \lesssim 0.4\,(0.2) \tag{3.27}$$

for $m_t \gtrsim 20$ (40) GeV. For the effective $Z'\bar{f}f$ vertex, the appropriate scalar $\phi_{Z'}$ is primarily a piece of an N supermultiplet (we need $x \gg v$ to get $m_{Z'} \gg m_Z$, and we assume here that $y = 0$) and $\Gamma_{\phi_{Z'}}$ will be dominated by the coupling of $\phi_{Z'}$ to a D-quark or squark. This means that there will be no light m_i^2 suppression factor, but there will be an extra, heavy propagator factor and thus probably no $\ln(m_D^2/m_i^2)$ enhancement. In addition, $(g^2 + g'^2)/m_Z^2 \to g_{Z'}^2/m_{Z'}$ in the effective four-fermion interaction, so we expect a form similar to (3.26), but with a coefficient

$$C' \sim \frac{\lambda_i^2 m_W^2}{m_{Z'}^2} \frac{G_F}{4\pi^2\sqrt{2}} \tag{3.28}$$

giving

$$\lambda_{6,7,9,10} \lesssim 0.2\left(m_{Z'}/300\,\text{GeV}\right) \tag{3.29}$$

For numerical purposes in the table, we take $m_{Z'} = 300$ GeV.

3.1.3 $K \to \pi\bar{\nu}\nu$

This is among the K processes listed in the table which are expected in the Standard Model, albeit with a rate far below the current experimental limit $B(K^+ \to \pi^+\bar{\nu}\nu) < 1.4 \times 10^{-7}$. Comparing this with the conventional decay rate [41] $B(K^+ \to \pi^0 e^+ \nu) \approx 4.8 \times 10^{-2}$, we infer that if

$$\mathcal{L}_{\text{eff}} = C_\nu (\bar{\nu}_L \gamma^\mu \nu_L)(\bar{s}_R \gamma_\mu d_R) \tag{3.30}$$

then

$$|C_\nu| < 1.7\times10^{-3} \times \frac{4G_F}{\sqrt{2}} \sin\theta_C \simeq 1.3\times10^{-8}\,\text{GeV}^{-2} \tag{3.31}$$

In this case we have no tree-level Higgs exchange contribution, since the $H^0\nu^c\nu$ couplings must be zero, or very nearly so, if we are to have acceptably small neutrino masses. Hence the absence of a (3,2) or (3,3) entry in the table. However, Z^0 exchange as in Fig. 6a can contribute through the D_L/d_L mixing mechanism discussed in subsection 3.1.1:

$$\mathcal{L}_{\text{eff}} \simeq \frac{g_L^2 + g'^2}{2m_Z^2} \epsilon_L^2 (\bar{\nu}_L \gamma^\mu \nu_L)(\bar{s}_L \gamma_\mu d_L) \tag{3.32}$$

Combining (3.31) and (3.32), we obtain

$$\frac{g_L^2 + g'^2}{m_Z^2} \epsilon_L^2 < 2.6\times10^{-8} \tag{3.33}$$

and hence the (3,9) entry in the table. As in the case of K^0–$\bar{K}^0$ mixing and $K_L \to \mu^+\mu^-$, the Z′ exchange gives similar bounds, shown in the (3,10) entry in the table. Figures 6b to 6d provide effective interactions

$$\mathcal{L}_{eff} \simeq \frac{\lambda_8^2}{m_D^2} \frac{1}{2}(\bar{\nu}_L \gamma^\mu \nu_L)(\bar{s}_L \gamma_\mu d_L), \frac{\lambda_{10}^2}{m_D^2} \frac{1}{2}(\bar{\nu}_L \gamma_\mu \nu_L)(\bar{s}_R \gamma^\mu d_R) \quad (3.34)$$

and a cross-term $\propto \lambda_8\lambda_{10}$ which is analogous to (3.13) and which we discard for the same reason. Combining (3.31) and (3.34), we obtain the (3,6) and (3,8) entries in the table.

The effective $s\bar{d}Z$ and $s\bar{d}Z'$ vertices will also give a contribution to $K \to \pi\bar{\nu}\nu$ via Fig. 5c with $\mu \to \nu$. Following the discussion in the previous section, we obtain

$$\lambda_{6,7}(t) \lesssim 1.2\ (1.8) \quad (3.35)$$

for $m_t \gtrsim 20$ (40) GeV from the t-exchange contribution to the effective $s\bar{d}Z$ vertex and

$$\lambda_{6,7,9,10} \lesssim 1.0\left(m_{Z'}/300\text{GeV}\right) \quad (3.36)$$

from the effective $s\bar{d}Z'$ vertex. These bounds would be improved by almost a factor of 10 by a measurement of the $K^+ \to \pi^+\bar{\nu}\nu$ branching ratio at the 10^{-10} level.

3.1.4 $K \to \pi e^+e^-$

This is the last of the K processes that are listed in the table and can occur in the Standard Model, and the branching ratio [41] for charged-kaon decay, $B(K^+ \to \pi^+e^+e^-) = (2.7 \pm 0.5) \times 10^{-7}$, is in order of magnitude agreement with theoretical expectation [38]. Again we assume conservatively that contributions from new physics amount to no more than a factor of 5 times the observed rate: $B_{new}(K^+ \to \pi^+e^+e^-) \lesssim 1.5 \times 10^{-6}$. Comparison with the allowed decay $B(K^+ \to \pi^0e^+\nu) \simeq 0.048$ that arises from the effective Lagrangian (3.16) (with $\mu \to e$) then implies that for

$$\mathcal{L}_{eff} = C_{ee}(\bar{e}_R \gamma_\mu e_R)(\bar{s}_R \gamma^\mu d_R) + h.c. \quad (3.37)$$

we must require (the ratio of matrix elements is $\sqrt{2}$)

$$|C_{ee}| < 4 \times 10^{-3} \times \frac{4G_F}{\sqrt{2}} \sin\theta_c \simeq 3 \times 10^{-8}\text{GeV}^{-2} \quad (3.38)$$

The Lagrangian (3.37) receives contributions from Fig. 5c (with $\mu \to e$). Comparison with (3.31) shows that the bounds for $\lambda_{6,7,8,9}$ from the effective $\bar{s}dZ$ and $\bar{s}dZ'$ vertices are about the same as those from $K \to \pi\bar{\nu}\nu$. However, the process also gets a contribution from the induced effective $\bar{s}d\gamma$ vertex. The full effective $\bar{f}f'\gamma$ vertex is of the form

$$f_1 \gamma_\mu (g^{\mu\nu} q^2 - q^\mu q^\nu) + f_2 \sigma^{\mu\nu} q_\mu \tag{3.39}$$

Only the charge radius $f_1 = \langle r^2 \rangle / 6$ contributes to $K^+ \to \pi^+ e^+ e^-$. Again it can be evaluated using (off-shell) Ward identities as in Ref. [38], and with appropriate substitutions ($m_W \to m_D$, $m_c \to m_i$, etc.) it is expected to be numerically similar to the GL result for charm exchange:

$$f_1 \simeq - Q_i \frac{e^2}{6\pi^2} \frac{\lambda^2}{4} \ln (m_D^2 / m^2) \tag{3.40}$$

where m^2 is the largest of the internal and external light fermion masses. In this case neutrino exchange cannot contribute (except through the photon coupling to the D, giving an additional heavy propagator suppression), so no useful limit is obtained for $\lambda_{9,10}$. For $\lambda_{6,7}$ the largest contribution is from u exchange: $m^2 = m_K^2$, $Q_i = 2/3$, giving

$$|C_{ee}| \simeq Q_i \frac{\alpha}{6\pi} \frac{1}{m_D^2} \lambda_{6,7}^2 \ln (m_D^2 / m^2) \simeq 4 \times 10^{-8} \lambda_{6,7}^2 \tag{3.41}$$

Comparison with the bound (3.38) gives the (4,4) and (4,5) entries in the table: $\lambda_{6,7} \lesssim 0.9$. CP conservation forbids [38] the decay $K_L \to \pi^0 \ell^+ \ell^-$ by the mechanism of Fig. 5c. The bound [41] $B(K_L \to \pi^0 e^+ e^-) < 2.3 \times 10^{-6}$ compared with $B(K_L \to \pi^\pm e^\mp \nu) = 0.39$ implies

$$|\sin\delta \, C_{ee}| < 2 \times 10^{-3} \sin\theta_c \times \frac{4 G_F}{\sqrt{2}} \tag{3.42}$$

where δ is a CP-violating parameter, so from the absence of $K_L \to \pi^0 e^+ e^-$ we obtain bounds on $\lambda_i \sqrt{\sin \delta_i}$ which are numerically similar to the bounds on λ_i from the charged mode.

The effective interaction (3.20) (with $\mu \to e$) can also contribute to $K^+ \to \pi^+ e^+ e^-$. In this case the matrix element enhancement relative to $K^+ \to \pi^0 e^+ \nu$ is roughly $m_K / m_s \simeq 3$ (with an extra factor of $\sqrt{2}$ for K^+ decay), and now $K_L^0 \to \pi^0 e^+ e^-$ is the CP-allowed neutral mode. Both modes give roughly the same bound:

$$\sqrt{\lambda_1 \lambda_2} \lesssim 8 \times 10^{-5} m_H \simeq 8 \times 10^{-3} \tag{3.43}$$

for $m_H \simeq 100$ GeV. Note, however, that in the Standard Model the coupling $\sqrt{\lambda_1 \lambda_2}$ relevant to this process is only $2\sqrt{m_e m_s}/250$ GeV $\approx 7 \times 10^{-4}$, so the bound (3.43) is weaker than the observed suppression of Yukawa couplings, which must nevertheless be accounted for in any model.

3.1.5 $K_L \to \mu e$

We assume the upper bound [42] $B(K_L \to \mu e) < 10^{-8}$ and imitate the discussion of subsection 3.1.2 to deduce (in an obvious notation) that

$$|C_{01}| < 1.3 \times 10^{-9} R^{-1} \text{ GeV}^{-2} \tag{3.44}$$

From the neutral Higgs diagram of Fig. 7 we obtain

$$\mathcal{L}_{eff} = \frac{\lambda_1\lambda_2}{m_H^2}(\bar{s}_R d_L)(\bar{\mu}_L e_R) \tag{3.45}$$

for which

$$R' = \frac{2m_K^2}{m_\mu m_s} \simeq 30 \tag{3.46}$$

Accordingly, we deduce

$$\frac{\lambda_1\lambda_2}{m_H^2} \lesssim 0.4\times10^{-10}\ \text{GeV}^{-2} \tag{3.47}$$

as exhibited across entries (5,2) and (5,3) of the table. There are no interesting Z^0 (Z') exchange contributions, because although there can be D_L/d_L (D_R/d_R) mixing, there is no leptonic flavour-changing Z^0 (Z') vertex at the tree level. Neither are there any interesting D/D^c exchange diagrams, since the only couplings of D/D^c and $\ell^\pm$ are to charge-2/3 quarks.

3.1.6 $K^+ \to \pi^+\mu e$

Here the relevant experimental bound [42] is $\Gamma(K^+ \to \pi^+\mu e)/\Gamma(K^+ \to \pi^0\mu^+\nu) < 1.7 \times 10^{-7}$, and we deduce again in an obvious notation that

$$|C_{0''}| < 8\times10^{-9} R''^{-1}\ \text{GeV}^{-2} \tag{3.48}$$

by analogy with (3.44). This bound is less restrictive because the upper limit on the exotic branching ratio is not competitive. The only contribution to this process is again from Fig. 7, so the relevant $\mathcal{L}_{\text{eff}}$ is in Eq. (3.45). Taking over the estimate (3.46) for the ratio R″ of matrix elements required in Eq. (3.55), we infer the (6,2) and (6,3) entries of the table. As in the previous subsection, there are no other interesting FCNIs in the superstring models under examination.

3.2 D physics

3.2.1 D^0–$\bar{D}^0$ *mixing*

Here the relevant experimental constraint is that [43] $\Gamma(\bar{D}^0 \to \mu^+X)/\Gamma(\bar{D}^0 \to \mu^-X) \leq 5.6 \times 10^{-3}$, implying

$$\left|\frac{\Delta m_D}{\Gamma_{D^0}}\right|^2 \lesssim 1.1\times10^{-2} \tag{3.49}$$

Taking

$$\Gamma_{D^0} \simeq 1.5\times10^{-12}\ \text{GeV} \tag{3.50}$$

we infer from the constraint (3.49) that

$$|\Delta m_D| \lesssim 1.5\times10^{-13}\ \text{GeV} \tag{3.51}$$

We assume that vacuum saturation is a good approximation to the matrix element of O'_{LL} in the effective interaction

$$\mathcal{L}_{eff} \equiv C'_{LL} O'_{LL} \equiv C'_{LL} (\bar{c}_L \gamma^\mu u_L)^2 \tag{3.52}$$

so that

$$\Delta m_D \simeq f_D^2 m_D C'_{LL} \tag{3.53}$$

where we guess that $f_D \simeq 0.2$ GeV. Inserting the experimental bound (3.51) into the expression (3.53) then yields

$$|C'_{LL}| \lesssim 2.1 \times 10^{-12} \text{ GeV}^{-2} \tag{3.54}$$

The enhancement of the matrix element of the $(\bar{s}_L \gamma^\mu d_L)$ $(\bar{s}_R \gamma^\mu d_R)$ operator over that of the $(\bar{s}_L \gamma^\mu d_L)$ $(\bar{s}_L \gamma_\mu d_L)$ operator assumed in subsection 3.1.1 could be traced to the relatively large ratio of m_K/m_s. We expect no analogous enhancement in the matrix element M_{LR} between D^0 and $\bar{D}^0$ of the corresponding $O'_{LR} \equiv (\bar{C}_L \gamma^\mu u_L)(\bar{C}_R \gamma^\mu u_R)$ operator

$$\frac{M_{LR}}{M_{LL}} \simeq \frac{3}{4}\left(\frac{m_D^2}{(m_c + m_u)^2} + \frac{1}{6}\right) \simeq 1 \tag{3.55}$$

and therefore take

$$|C'_{LR}| \lesssim 2.1 \times 10^{-12} \text{ GeV}^{-2} \tag{3.56}$$

as the appropriate bound on its magnitude.

The Higgs exchange diagram of Fig. 8a gives an effective interaction,

$$\mathcal{L}_{eff} = \frac{\lambda_1^2}{m_H^2} (\bar{C}_R u_L)(\bar{C}_L u_R) = \frac{\lambda_1^2}{2m_H^2} (\bar{C}_R \gamma^\mu u_R)(\bar{C}_L \gamma_\mu u_L) \tag{3.57}$$

which we combine with (3.56) to give the (6,1) entry in the table. There are no tree-level Z^0 or Z' exchange contributions, because there is no mixing of the u-quarks analogous to the D/d mixing discussed in subsection 3.1.1. Turning to the loop diagrams of Figs. 8b to 8d, we find that the D and $\tilde{D}$ exchanges of Fig. 8b give

$$\mathcal{L}_{eff} \sim \text{either } \frac{\lambda_6^4}{64\pi^2} \frac{1}{2m_D^2} (\bar{C}_L \gamma^\mu u_L)^2 \text{ or } \frac{\lambda_9^4}{64\pi^2} \frac{1}{2m_D^2} (\bar{C}_R \gamma^\mu u_R)^2 \tag{3.58}$$

while the D^c and $\tilde{D}^c$ exchanges of Fig. 8c give

$$\mathcal{L}_{eff} \sim \text{either } \frac{\lambda_7^4}{64\pi^2} \frac{1}{2m_{D^c}^2} (\bar{C}_R \gamma^\mu u_R)^2 \text{ or } \frac{\lambda_8^4}{64\pi^2} \frac{1}{2m_{D^c}^2} (\bar{C}_L \gamma^\mu u_L)^2 \tag{3.59}$$

As in the case of Fig. 4e, the D/D^c mixing diagram in Fig. 8d has a complicated dependence on combinations of unknown parameters, and would in any case not give a more stringent bound. Equations (3.58) and (3.59) combined with the bound (3.54) give the entries (7,4/5/6/7) in the table.

3.2.2 $D^0 \to \mu^+\mu^-$

An experimental upper limit on this decay has recently appeared [43]:

$$B(D^0 \to \mu^+\mu^-) < 1.1 \times 10^{-5} \tag{3.60}$$

If, from the lifetime measurement, we take the total D^0 decay width to be

$$\Gamma(D^0 \to \text{all}) \simeq 1.5 \times 10^{-12}\ \text{GeV} \tag{3.61}$$

the upper limit (3.60) yields

$$\Gamma(D^0 \to \mu^+\mu^-) \lesssim 1.6 \times 10^{-17}\ \text{GeV} \tag{3.62}$$

which we will now compare with the possible superstring contributions to this decay.

The Higgs diagram of Fig. 9a can give an effective interaction,

$$\mathcal{L}_{\text{eff}} = \frac{\lambda_1\lambda_2}{m_H^2}(\bar{c}_R u_L)(\bar{\mu}_R \mu_L) \tag{3.63}$$

where we have assumed that the $H\bar{H}$ mixing term provided by the $\lambda_4\, H\bar{H}N$ term, $\mu = \lambda_4 x$, is of the same order as the diagonal terms in the $(H, \bar{H})$ mixing matrix. The operator (3.63) does not have any helicity suppression in its matrix element, and we estimate that (3.63) gives

$$\Gamma(D^0 \to \mu^+\mu^-) \simeq \left(\frac{\lambda_1\lambda_2}{m_H^2}\right)^2 \times (1.3 \times 10^{-3}\ \text{GeV}^5) \tag{3.64}$$

where we have again used $f_D \approx 0.2$ GeV. Comparing (3.62) and (3.64), we deduce the joint (8,1) and (8,2) entry in the table. The D and D^c exchange diagrams of Fig. 9b provide effective interactions of the form

$$\mathcal{L}_{\text{eff}} \simeq \frac{\lambda_B^2}{2m_{D^c}^2}(\bar{u}_L\gamma^\mu c_L)(\bar{\mu}_L\gamma_\mu\mu_L) + \frac{\lambda_{q_2}^2}{2m_{\tilde{D}}^2}(\bar{u}_R\gamma^\mu c_R)(\bar{\mu}_R\gamma_\mu\mu_R) \tag{3.65}$$

in the case of the superpotential (2.19). However, the matrix elements of these two operators are helicity suppressed, so we obtain no interesting results for the (8,6) and (8,7) entries in the table.

3.2.3 $D^0 \to \mu^\pm e^\mp$

Experimental upper limits on this decay have recently been quoted [44] and a more stringent one is soon to be published [45]:

$$B(D^0 \to \mu e) \lesssim 1.5 \times 10^{-4} \tag{3.66}$$

Combined with the total D^0 decay width (3.61), this gives

$$\Gamma(D^0 \to \mu e) \lesssim 2.3 \times 10^{-16}\ \text{GeV} \tag{3.67}$$

If we use the same assumptions as those used in the previous subsection for $H\bar{H}$ mixing, in this case the Higgs diagram of Fig. 9a can give an effective interaction

$$\mathcal{L}_{eff} = \frac{\lambda_1\lambda_2}{m_H^2}(\bar{c}_R u_L)(\bar{\mu}_R e_L) \tag{3.68}$$

which, as before, for $f_D \approx 0.2$ GeV yields the estimate

$$\Gamma(D^0 \to \mu e) \simeq \left(\frac{\lambda_1\lambda_2}{m_H^2}\right)^2 \times (1.3 \times 10^{-3}\,\mathrm{GeV}^5) \tag{3.69}$$

Comparing (3.67) and (3.69) we deduce the joint (9,1) and (9,2) entry in the table. The D and D^c exchange diagrams of Fig. 9b provide interactions of the form

$$\mathcal{L}_{eff} \simeq \frac{\lambda_8^2}{2m_{\tilde{D}^c}^2}(\bar{u}_L\gamma^\mu c_L)(\bar{e}_L\gamma_\mu\mu_L) + \frac{\lambda_9^2}{2m_{\tilde{D}}^2}(\bar{u}_R\gamma^\mu c_R)(\bar{e}_R\gamma_\mu\mu_R) \tag{3.70}$$

for the superpotential (2.19).

However, the matrix elements of these operators are helicity-suppressed, and we obtain only the very weak bounds $\lambda_{8,9} < 2$ for the (9,6) and (9,7) entries in the table.

3.2.4 $D^0 \to \mu^\pm e^\mp X$

No experimental upper limit on this decay has yet been quoted, but present experimental data could perhaps be used to establish a limit comparable to (3.60), or perhaps somewhat worse. The relevant effective operators are again (3.63) generated by Higgs exchange and (3.65) generated by D and D^c exchanges. In the case of this inclusive decay there is no possibility of helicity suppression to be concerned about, and we estimate

$$8G_F^2\,\frac{\Gamma(D^0 \to \mu e X)}{\Gamma(D^0 \to \mu\nu X)} \simeq \left(\frac{\lambda_1\lambda_2}{m_H^2}\right)^2, \left(\frac{\lambda_8^2}{2m_{\tilde{D}^c}^2}\right)^2, \left(\frac{\lambda_9^2}{2m_{\tilde{D}}^2}\right)^2 \tag{3.71}$$

Taking 10^{-3} as an attainable upper bound for $B(D^0 \to \mu eX)$, and 7×10^{-2} for $B(D \to \mu\nu X)$, we arrive at

$$\frac{\lambda_1\lambda_2}{m_H^2}, \frac{\lambda_8^2}{2m_{\tilde{D}^c}^2}, \frac{\lambda_9^2}{2m_{\tilde{D}}^2} \lesssim 1.8 \times 10^{-1} \times \left(\frac{4G_F}{\sqrt{2}}\right) \tag{3.72}$$

The resulting bounds on λ_1, λ_3, λ_8, and λ_9 are not very interesting, but for completeness they are listed with question marks in entries (10,1), (10,2), (10,6), and (10,7) of the table.

3.3 B physics

3.3.1 B^0–$\bar{B}^0$ mixing

Experimental upper limits [46] on B^0–$\bar{B}^0$ mixing have recently become available, telling us that

$$\frac{1}{2}\left(\frac{\Delta m_B}{\Gamma_B}\right)^2 \lesssim 0.12 \tag{3.73}$$

Taking $\Gamma_B \approx 1.42 \times 10^{-12}\,\mathrm{s}^{-1}$ also from experiment, we therefore infer that

$$|\Delta m_B| \lesssim 2.3 \times 10^{-13}\ \text{GeV} \tag{3.74}$$

which is starting to be comparable with the observed value of Δm_K and the upper limit on Δm_D (3.51). Parallelling the analysis of subsection 3.2.1, we see that the effective interactions

$$\mathcal{L}_{\text{eff}} = \begin{cases} C''_{LL} O''_{LL} & : O''_{LL} \equiv (\bar{b}_L \gamma^\mu d_L)^2 \\ C''_{LR} O''_{LR} & : O''_{LR} \equiv (\bar{b}_L \gamma^\mu d_L)(\bar{b}_R \gamma_\mu d_R) \end{cases} \tag{3.75}$$

and the estimates

$$\Delta m_B \simeq f_B^2 m_B^2 C''_{LL,LR} \tag{3.76}$$

lead to the bounds

$$|C''_{LL}|, |C''_{LR}| \leq 1.1 \times 10^{-12}\ \text{GeV}^{-2} \tag{3.77}$$

The diagrams contributing to this process are identical with those for K^0–$\bar{K}^0$ mixing. The Higgs exchange diagram of Fig. 4a gives an O''_{LR} operator, whilst Fig. 4b generates an O''_{LL} operator. Figures 4c and 4d also give O''_{LL} operators, whilst Fig. 4e gives an O''_{LR} operator. All the coefficients have the same forms as in Eqs. (3.6), (3.9), (3.9.1), and (3.11) to (3.13), so the upper bounds (3.77) immediately lead to the entries (11,3/4/5) and (11,7/8/9/10) in the table.

3.3.2 B_S^0–$\bar{B}_S^0$ mixing

There is no significant upper limit on this mixing, which is in any case expected to be maximal in the Standard Model. Therefore, we have not considered in detail the contributing diagrams analogous to Fig. 4.

3.3.3 $B \to \mu^+\mu^- X$, $B \to e^+e^- X$

There are upper limits on these decays at the level of [41]

$$B(B \to \mu^+\mu X \text{ or } e^+e^- X) \lesssim 6 \times 10^{-3} \tag{3.78}$$

to be compared with the standard semileptonic decay branching ratios

$$B(B \to \mu\nu X \text{ or } e\nu X) \simeq 0.12 \tag{3.79}$$

Although the bounds on Yukawa couplings coming from (3.78) are much weaker than those on the analogous couplings from $K^+ \to \pi^+e^+e^-$ decay, in principle the limits (3.78) probe the couplings of different fermion generations, and are thus of some interest. We can compare the Standard Model four-fermion operator for semileptonic $b \to c\ell\nu$ decay:

$$\mathcal{L}_{SM} = \frac{4G_F}{\sqrt{2}} (\bar{b}_L \gamma^\mu c_L)(\bar{l}_L \gamma_\mu \nu_L) S_\Theta \tag{3.80}$$

where s_θ is the appropriate Cabibbo–Kobayashi–Maskawa matrix element, with the operator due to Higgs exchange:

$$\mathcal{L}_H = \frac{\lambda_2\lambda_3}{m_H^2}(\bar{\nu}_R c_L)(\bar{\nu}_L \ell_R) \tag{3.81}$$

Using (3.78) and (3.79), we find the upper bound

$$\sqrt{\lambda_2\lambda_3} < 0.06 \tag{3.82}$$

Although this is much weaker than the other bounds listed in columns 2 and 3 of the table, there is the possibility of substantial experimental improvement in the upper limit (3.78).

3.3.4 $B \to e^+e^-, \quad e^\pm\mu^\mp, \quad \mu^+\mu^-, \quad K\ell^+\ell^-$

These are the only exclusive flavour-changing decays of B mesons for which upper limits [47] have been quoted (0.8×10^{-4}, 0.9×10^{-4}, 0.9×10^{-4}, and 2.1 to 6.5×10^{-4}, respectively). They would receive contributions from diagrams analogous to Fig. 5, but we do not present detailed results because the corresponding rare K decays are more sensitive probes of these classes of interactions.

3.4 Muon physics

3.4.1 $\mu N \to eN$

The most sensitive upper limit on this process is from $\mu \to$ e conversion on titanium [48]:

$$\frac{\Gamma(\mu^- \mathrm{Ti} \to e^- \mathrm{Ti})}{\Gamma(\mu^- \mathrm{Ti} \to \nu_\mu X)} \lesssim 6 \times 10^{-12} \tag{3.83}$$

The Standard Model interaction contributing to $\mu^- \to \nu_\mu$ conversion is

$$\mathcal{L}_{\mathrm{eff}} = \frac{g_2^2}{2m_W^2}(\bar{\nu}_L \gamma^\mu \mu_L)(\bar{d}_L \gamma_\mu c) \tag{3.84}$$

which acts coherently on the nucleus through the vector piece of the left-handed quark coupling. Scalar couplings to quarks also act coherently on the nucleus, and the upper bound on the coefficient C_V and C_S of any such vector or scalar interaction deduced from (3.83) and (3.84) is

$$C_{V,S} \lesssim 0.7 \times 10^{-10}\ \mathrm{GeV}^{-2} \tag{3.85}$$

Coherent contributions can be obtained from the diagrams of Fig. 10. Higgs exchange as in Fig. 10a gives an interaction

$$\mathcal{L}_{\mathrm{eff}} = \frac{\lambda_2\lambda_3}{m_{\bar{H}}^2}(\bar{d}_L d_R)(\bar{e}_R \mu_L) \tag{3.86}$$

There would be a similar contribution $\propto \lambda_1\lambda_2$ from Fig. 10b if $H\bar{H}$ mixing due to the $\lambda_4 H\bar{H}N$ coupling in (2.19) were maximal, but we do not consider it in view of the additional uncertainties. The exchanges of scalar $\tilde{D}$ and $\tilde{D}^c$ fields as in Fig. 10c give (after Fierz transformation)

$$\mathcal{L}_{eff} \simeq \begin{cases} \frac{\lambda_8^2}{2m_{D^c}^2} (\bar{u}_L \gamma^\mu u_L)(\bar{e}_L \gamma_\mu \mu_L) \\ \frac{\lambda_9^2}{2m_{D^c}^2} (\bar{u}_R \gamma^\mu u_R)(\bar{e}_R \gamma_\mu \mu_R) \end{cases} \tag{3.87}$$

There could also be contributions from analogous diagrams with D/D^c mixing, which we also discard in view of the extra uncertainties involved. Estimating that the effective interactions (3.84), (3.86), and (3.87) all have similar coherent nuclear matrix elements, we obtain the (12,2) (12,3), (12,6), and (12,7) entries in the table.

3.4.2 $\mu \to eee$

The best upper limit on the branching ratio for this decay [49] is

$$B(\mu \to eee) \leq 8 \times 10^{-13} \tag{3.88}$$

This is to be compared with the branching ratio calculated [50] using the general matrix element for helicity-flip amplitudes:

$$\mathcal{M} = C_{ab}\left(\bar{u}_e(k_1)(1-a\gamma_5)u_\mu(p)\right)\left(\bar{u}_e(k_2)(1-b\gamma_5)v_e(k_3)\right) - (k_1 \leftrightarrow k_2) \tag{3.89}$$

which is

$$B(\mu \to eee) = \frac{|C_{ab}|^2}{8G_F^2}(2A+B) \tag{3.90}$$

where

$$\left.\begin{aligned} A &= 3(1+a^2)(1+b^2) + 4ab \\ B &= (1+a^2)(1+b^2) + 4ab \end{aligned}\right\} \tag{3.91}$$

The first contribution to $\mu \to eee$ that we consider is due to the Higgs exchange diagram of Fig. 11a, which provides

$$\mathcal{L}_{eff} = \frac{\lambda_2^2}{m_H^2}(\bar{e}_L e_R)(\bar{e}_R \mu_L) \tag{3.92}$$

corresponding to a = 1, b = −1:

$$A = 8, \quad B = 0, \quad C_{1-1} = \frac{\lambda_2^2}{4m_H^2} \tag{3.93}$$

Inserting (3.93) into (3.90) and using the experimental upper limit (3.88) we obtain the (13,2) entry in the table. There is also a possible contribution from the D and/or D^c loop diagrams of Figs. 11b to 11d. As in subsection 3.4.1, we neglect D/D^c mixing, and retain

$$\mathcal{L}_{eff} \simeq \begin{cases} \frac{\lambda_8^4}{64\pi^2} \frac{1}{2m_D^2} (\bar{e}_L \gamma^\mu \mu_L)(\bar{e}_L \gamma_\mu e_L) \\ \frac{\lambda_9^4}{64\pi^2} \frac{1}{2m_D^2} (\bar{e}_R \gamma^\mu \mu_R)(\bar{e}_R \gamma_\mu e_R) \end{cases} \tag{3.94}$$

Since these are pure V ∓ A interactions, they can be directly compared with $\mu \to e\nu\bar{\nu}$, which when combined with the bound (3.88) gives $\lambda_{8,9} < 0.3$.

More stringent bounds can be obtained by considering the $\bar{\mu}eV$ (V = Z, Z′,γ) vertex, i.e. the analogue of Fig. 5c with s, d → μ, e; μ, e; μ, μ → e, e. These diagrams also probe $\lambda_{8,9}$. Following the discussion in subsections 3.1.2–4 we recall that Z-exchange requires the t-quark to be significant, whilst γ-exchange is most important for a light, charged fermion. These exchanges induce effective four-fermion Lagrangians of the form

$$\mathcal{L}_{eff} = \sum_{h,h'} (C_{\mu e 3})_{hh'} (\bar{\mu}_h \gamma^\mu e_h)(\bar{e}_{h'} \gamma_\mu e_{h'}) \tag{3.95}$$

(h, h′ = L or R) which after Fierz rearrangement is a linear combination of (3.89) and (3.94) with the relative coefficient and a, b in (3.89) depending on the Clebsch–Gordan coefficients for γ, Z, Z′ couplings. In the following we treat all these O(1) coefficients as unity and assume, using (3.88), that

$$|(C_{\mu e 3})_{hh'}| \lesssim (8 \times 10^{-13})^{1/2} \times \frac{4G_F}{\sqrt{2}} \simeq 3 \times 10^{-11}\ \text{GeV}^{-2} \tag{3.96}$$

for each pair hh′. We will also neglect Z′ exchange since Z + t exchange and γ + u,c exchange yield stronger bounds for all the relevant $\lambda_{8,9}$. From Eq. (3.26) in subsection 3.1.2, we see that Z + t exchange ($m_i = m = m_t$) gives

$$|C_{\mu e 3}| \sim \frac{\lambda_{8,9}^2}{m_D^2} \frac{m_t^2 G_F}{4\pi\sqrt{2}} \ln(m_D^2/m_t^2) \tag{3.97}$$

yielding the bound: $\lambda_{8,9} < 0.08$ (0.05) for $m_t > 20$ GeV (40 GeV). Similarly, Eq. (3.40) for γ + u exchange ($Q_i = 2/3$, $m = m_\mu$) gives

$$|C_{\mu e 3}| \sim \lambda_{8,9}^2 \frac{\alpha}{6\pi} \frac{1}{m_D^2} \ln(m_D^2/m_\mu^2) \tag{3.98}$$

yielding $\lambda_{8,9} < 0.02$. The bound for γ + c exchange is weaker by a factor $[\ln(m_D/m_c)/\ln(m_D/m_\mu)]^{1/2} \approx 1.3$, i.e. $\lambda_{8,9} < 0.03$—hence the entries (13,6) and (13,7) in the table. These bounds are much stronger than those obtainable from the contributions $\propto \lambda^4/m_D^4$ which were discussed earlier in this subsection. (The same remark applies to analogous contributions to the processes discussed in previous subsections.)

3.4.3 $\mu \to e\gamma$

The best upper limit [51] for this branching ratio is

$$B(\mu \to e\gamma) \leq 4.9 \times 10^{-11} \tag{3.99}$$

One-loop interactions may contribute to this decay by generating an effective anomalous magnetic moment interaction of the form

$$\mathcal{L}_{eff} = e \frac{a}{4m_\mu} F^{\mu\nu} \bar{e}_{R_L} \sigma_{\mu\nu} \mu_{L_R} \tag{3.100}$$

which (3.99) bounds by

$$a \lesssim 2.4 \times 10^{-13} \tag{3.101}$$

Contributing one-loop diagrams are shown in Fig. 12. Higgs exchange as in Fig. 12a yields

$$a \simeq \frac{m_\mu^2}{m_H^2} \frac{\lambda_1^2}{4\pi^2} \ln(m_H^2/m^2) \tag{3.102}$$

where m is again the largest of internal and external light fermion masses. We compare (3.101) and (3.102) to obtain the (14,2) entry which corresponds to the largest possible enhancement (internal electron or muon: $m = m_\mu$),

$$\lambda_1 < 8 \times 10^{-4} \tag{3.103}$$

for $m_H = 100$ GeV. The bound corresponding to τ exchange is weakened by a factor of 1.6. The exchanges of D or D^c fields as in Fig. 12b yield an expression analogous to (3.102), with m_H^2 replaced by $3/2\, m_D^2$ or $m_{D^c}^2$ because of the u-quark charge. The bound for u exchange ($m = m_\mu$) is

$$(\lambda_8^2 + \lambda_9^2)^{1/2} \lesssim 3 \times 10^{-3} \tag{3.104}$$

for $m_D = m_{D^c} = 300$ GeV, which is weakened by factors of 1.2 and about 4 [$\ln(m_H/m_Z) \approx 1$] for c- and t-quark exchange, respectively.

It is worth noting that if there is substantial D–D^c mixing, the t-quark contribution can be significantly enhanced by the diagram of Fig. 12c, which does not require a mass insertion on the external muon line. This gives an enhancement factor $(m_t^2/m_\mu^2)\Delta$, where $\Delta = m_{DD^c}^2/m_D^2$ yielding the bound:

$$\sqrt{\Delta}\lambda_8\lambda_9 \lesssim 6 \times 10^{-5} \tag{3.105}$$

for $m_t \gtrsim 20$ GeV.

3.4.4 The muon anomalous magnetic moment

Although this is hardly a rare process, we include a discussion of $(g-2)_\mu$ here because it is often a sensitive probe of new physics. However, it does not give significant constraints on the new type of superstring physics which we are discussing in this paper, as we now see. There are four potentially important superstring diagrams contributing to $(g-2)_\mu$ which are shown in Fig. 13. The Z′-exchange

diagram of Fig. 13a is always smaller than the Z^0 exchange diagram, which is itself smaller than the present experimental error bars. The neutral scalar-exchange diagram of Fig. 13b has the same structure as the $\widetilde{W}^{\pm}$ exchange diagram of the minimal supersymmetric Standard Model. This has been shown [52] to provide a lower bound on the $\tilde{\nu}$ mass of order 20 GeV for very light $\widetilde{W}^{\pm}$. Correspondingly, a Yukawa coupling as large as the SU(2) gauge coupling g_2 would be acceptable as long as $m_H \gtrsim 20$ GeV, and an even larger Yukawa coupling would be allowed for our reference choice $m_H = 100$ GeV. The charged Higgs-exchange diagram of Fig. 13c has the same structure as that of the $\widetilde{Z}^0$-exchange diagram of the minimal supersymmetric Standard Model, and is again much smaller than the experimental errors if the Yukawa coupling is $\leq g_2$ and $m_H = 100$ GeV. Finally, the D-exchange diagrams of Fig. 13d can be related to a linear superposition of the previous two, and are again negligible if $m_D = 300$ GeV, the general comparison value we assume. We conclude that $(g-2)_\mu$ does not provide useful constraints on superstring model parameters.

3.4.5 Radiative hyperon decay

It is amusing to note that if some of the λ_i were large the induced $\bar{s}d\gamma$ magnetic couplings would give observable contributions to radiative hyperon decay. Hyperon non-leptonic decay amplitudes are typically of order $m_\pi^2 G_F \sin^2\theta_C$. A magnetic $BB'\gamma$ coupling

$$\mathcal{L}_{eff} \sim \frac{e a}{4 m_s} F^{\mu\nu} \bar{B} \sigma_{\mu\nu} B + h.c. \tag{3.106}$$

gives an effective amplitude of order

$$e \frac{a}{4 m_s} |m_B - m_{B'}| \sim e \frac{a}{4 m_s} m_\pi \lesssim 10^{-3/2} \sin\theta_c m_\pi^2 G_F \tag{3.107}$$

since radiative hyperon decay branching ratios are measured to be or are bounded by $O(10^{-3})$. Thus we require

$$a \lesssim \frac{4}{e} m_s m_\pi \sin\theta_c 10^{-3/2} G_F \simeq 1.4 \times 10^{-7} \tag{3.108}$$

for $m_s \simeq 150$ MeV. Following the discussion of subsection 3.4.3 on $\mu \to e\gamma$, it is easy to see that we get the following contributions a(AB) to a, where A and B are the particles in the loop diagrams analogous to those of Fig. 12, and we assume $a_{BB'\gamma} \approx a_{sd\gamma}$:

$$a(Hd) \sim a(\bar{H}d^c) \sim a(Hs) \sim a(\bar{H}s^c) \sim \frac{m_s^2}{m_H^2} \frac{\lambda_{2,3}^2}{4\pi^2} \ln(m_H^2/m_s^2) \tag{3.109a}$$

$$a(H\bar{H}b) \sim \frac{m_b^2}{m_H^2} \Delta_H \frac{\lambda_2 \lambda_3}{4\pi^2} \ln(m_H^2/m_b^2) \tag{3.109b}$$

$$a(D\bar{u}) \sim a(D^c u^c) \sim 1{\cdot}6\, a(D\bar{c}) \sim 1{\cdot}6\, a(D^c c^c)$$
$$\sim \frac{2}{3} m_s^2/m^2_{D(D^c)} \frac{\lambda^2_{6,7}}{4\pi^2} \ln(m_D^2/m_s^2) \qquad (3.109c)$$

$$a(D\bar{D}^c t) \sim \frac{2}{3} \frac{m_t^2}{m_D^2} \Delta_D \frac{\lambda_6 \lambda_7}{4\pi^2} \ln(m_s^2/m_t^2) \qquad (3.109d)$$

where the second (fourth) contribution requires H–$(\bar{H})^\dagger$ [D–$(D^c)^\dagger$] mixing as in Fig. 12c:

$$\Delta_H = m^2_{H\bar{H}}/m^2_H \qquad (3.110)$$

$$\Delta_D = m^2_{D\bar{D}^c}/m^2_D \qquad (3.111)$$

Note that we could well have $\Delta_H = O(1)$. The above estimates provide the bounds, for $m_H = 100$ GeV, $m_D = m_{D^c} = 300$ GeV, $m_t \geq 20$ GeV:

$$\left.\begin{aligned} \lambda_{2,3} &\leq 0{\cdot}4, \ \sqrt{\Delta_H \lambda_2 \lambda_3} < 0{\cdot}04 \\ \lambda_{6,7} &< 1{\cdot}5, \ \sqrt{\Delta_D \lambda_6 \lambda_7} < 0{\cdot}02 \end{aligned}\right\} \qquad (3.112)$$

These bounds have not been quoted in the table, as they do not appear to be very competitive.

3.5 CP violation

3.5.1 Im $(K^0$–$\bar{K}^0)$

This is the only evidence for CP violation yet obtained. In Eqs. (3.4) and (3.5) we have already displayed corresponding upper bounds on the coefficients (Im $C_{LL,LR}$). The relevant diagrams are those in Fig. 4, which were discussed in subsection 3.1.1. The corresponding upper bounds on the couplings in the superstring superpotential (2.19) are displayed in entries (16,3/4/5) and (16,7/8/9/10) of the table. These entries often appear to be much more stringent than others in the same columns, but caution should be exercised in interpreting this result. This and other CP-violating quantities measure phases in Yukawa coupling matrices which are *a priori* independent of the real parts which dominate other processes. We will return to this point in the discussion in Section 4.

3.5.2 ϵ'/ϵ

There are two recent experimental upper measurements of this quantity

$$\epsilon'/\epsilon = \begin{cases} 0{\cdot}0017 \pm 0{\cdot}0082 & \text{(Ref. [53])}, \\ -0{\cdot}0046 \pm 0{\cdot}0053 \pm 0{\cdot}0024 & \text{(Ref. [54])}, \end{cases} \qquad (3.113)$$

from which we infer

$$|\epsilon'/\epsilon| < 0{\cdot}01 \qquad (3.114)$$

This quantity receives contributions from the Standard Model W penguin diagrams of Fig. 14a, which may well predict a value of $|\epsilon'/\epsilon|$ close to the upper limit (3.114). To be conservative, we neglect these contributions, and compare (3.114) directly with the novel superstring contributions. Tree-level Higgs exchange as in Fig. 14b gives an effective interaction,

$$\mathcal{L}_{eff} = \frac{\lambda_3^2}{m_H^2} (\bar{d}_L s_R)(\bar{d}_R d_L) \tag{3.115}$$

whilst the one-loop Higgs penguin diagram of Fig. 14c gives

$$\mathcal{L}_{eff} \simeq \frac{\lambda_3^2 g_3}{32\pi^2} m_s \bar{d}_L \sigma^{\mu\nu} F_{\mu\nu} s_R \tag{3.116}$$

There are also tree-level contributions from scalar D and D^c exchanges as in Fig. 14d and 14e (we neglect D/D^c mixing as usual) which after Fierz transformations yield

$$\mathcal{L}_{eff} = \begin{cases} \frac{\lambda_6^2}{2m_D^2} (\bar{d}_L \gamma^\mu u_L)(\bar{u}_L \gamma_\mu s_L) \\ \frac{\lambda_7^2}{2m_{D^c}^2} (\bar{d}_R \gamma^\mu u_R)(\bar{u}_R \gamma_\mu s_R) \end{cases} \tag{3.117}$$

and one-loop D penguin diagrams as in Fig. 14f which yield

$$\mathcal{L}_{eff} \simeq \frac{\lambda_6^2, \lambda_7^2}{32\pi^2} g_3 m_s \bar{d}_{L,R} \sigma^{\mu\nu} F_{\mu\nu} s_{R,L} \tag{3.118}$$

To estimate the contributions of the effective interactions [(3.115) to (3.118)] to ϵ'/ϵ we follow the examples of previous calculations in other models which led to similar operators.

The operators [(3.115) to (3.118)] have chiral structures similar to those appearing in the Weinberg model [55] of CP violation. It has been pointed out [56] that ϵ'/ϵ in this model is expected to be much smaller than had previously been thought, because of a cancellation between the diagrams of Figs. 14g and 14h. This cancellation occurs because in the Weinberg model

$$\begin{aligned} \langle K_S | \mathcal{L}_W | \pi^0 \pi^0 \rangle_{\text{fig. 14g}} &= -\frac{1}{f_\pi^2} \langle K_S | [Q_3^5, [Q_3^5, \mathcal{L}_W]] | 0 \rangle \\ &= -\frac{1}{4 f_\pi^2} \langle K_S | \mathcal{L}_W | 0 \rangle \end{aligned} \tag{3.119}$$

where Q_3^5 is the axial isospin charge with the quantum numbers of the π^0. It is easy to check that the same relation (3.119) holds for the operators (3.115) to (3.118), and hence that there is a chiral cancellation in the full CP-violating $K_S \to \pi^0\pi^0$ amplitude. There remains an η' pole contribution which is difficult to calculate reliably. In the Weinberg model this was estimated [56] to yield

$$\epsilon'/\epsilon = -0.006 \times (3^{0\pm1}) \tag{3.120}$$

which is certainly compatible with the experimental limit (3.114). We expect this estimate to be valid qualitatively for any model in which (3.119) holds and the same operator generates CP violation in

both the direct $K \to 2\pi$ amplitude and also in the K^0-$\bar{K}^0$ mixing matrix through the η' pole. Therefore the estimate (3.120) also applies to our operators (3.112) to (3.118), and there is no significant bound on the Yukawa couplings from considerations of ϵ'/ϵ. If we knew how to calculate reliably the real parts of the $K \to 2\pi$ decay amplitudes given by a specified $\Delta S = 1$ operator, we could use their experimental values to constrain λ_2, λ_6, and λ_7. However, we do not feel confident enough in our understanding of weak matrix elements to attempt such an exercise.

3.5.3 μ polarization in $K^0 \to \pi^- \mu^+ \nu$

To set up our calculation, we first review the standard theory [57] of this effect, then introduce the available experimental information, and finally estimate the possible superstring contributions. In the Standard Model, the $K_{\mu 3}$ decay amplitude is

$$\frac{G_F}{\sqrt{2}} \left[(\bar{\nu}_L \gamma^m \mu_L)(p_K + p_\pi)_\mu f_+ - (\bar{\nu}_L \mu_R) f_- m_\mu \right] \tag{3.121}$$

which cannot give a CP-violating μ polarization. However, if we have a scalar exchange interaction of the form

$$\mathcal{L}_{eff} = C_{SK} (\bar{s}_L u_R)(\bar{\nu}_L \mu_R) \tag{3.122}$$

then there is a CP-violating effect $\propto$ Im C_{SK}. The matrix element of $\mathcal{L}_{eff}$ (3.122) is given by current algebra:

$$\langle \pi^0 | \bar{s}_L u_R | K^+ \rangle = - a_S m_K \; ; \; a_S = \frac{(m_K^2 - m_\pi^2) f_+ - (p_\nu + p_\mu)^2 f_-}{(m_s - m_d) m_K} \tag{3.123}$$

Using SU(3) and CVC theory, we have $f_+ = 1/\sqrt{2}$, $f_- = 0$ at $q^2 = (p_\nu + p_\mu)^2 = 0$: experimentally, f_- is indeed much smaller than f_+. Then, taking $(m_s - m_d) \simeq 150$ MeV in Eq. (3.123), we deduce $a_S \simeq 2.2$. The muon polarization parameter is

$$\xi = \frac{f_- + \dfrac{a_S m_K}{m_\mu \sin\theta_C} \bar{C}_{SK}}{f_+} \tag{3.124}$$

where we defined a reduced coefficient $\bar{C}_{SK} = C_{SK}/(G_F/\sqrt{2})$, giving the CP-violating polarization

$$\mathrm{Im}\,\xi = \mathrm{Im}\,\bar{C}_{SK} \frac{a_S m_K}{m_\mu \sin\theta_C} \tag{3.125}$$

Experiment [58] tells us that

$$\mathrm{Im}\,\xi = 0.012 \pm 0.026 \Rightarrow |\mathrm{Im}\,\xi| < 0.04 \tag{3.126}$$

Inserting this bound into the expression (3.125), we deduce

$$|\mathrm{Im}\,\bar{C}_{SK}| < 5 \times 10^{-4} \tag{3.127}$$

The Higgs exchange diagram of Fig. 15a does indeed give us an operator of the type (3.122), with the coefficient

$$C_{SK} = \frac{\lambda_2 \lambda_3}{m_H^2} \tag{3.128}$$

Inserting the estimate (3.128) into the bound (3.127) gives us the (18,2/3) entry in the table. Scalar D and D^c exchanges as in Figs. 15b and 15c, after Fierz transformations, give effective interactions

$$\mathcal{L}_{eff} = \begin{cases} \frac{\lambda_9^2}{2m_D^2} (\bar{s}_L \gamma^\mu u_L)(\bar{\nu}_L \gamma_\mu \mu_L) \\ \frac{\lambda_8 \lambda_{10}}{2m_D^2} (\bar{s}_R \gamma^\mu u_R)(\bar{\nu}_R \gamma_\mu \mu_R) \end{cases} \tag{3.129}$$

which could induce a small phase δ in f_+ and hence $|\mathrm{Im}\ \xi| \propto |\sin \delta f_-|$. We expect this effect to be negligibly small. Contributions with a scalar structure could arise from D/D^c mixing as in Fig. 15d, but in view of the uncertainties in the amount of this mixing which have been discussed previously, we do not think it worth while to quote any limits on the basis of Fig. 15d.

3.5.4 Neutron electric dipole moment

The latest experimental determinations of this quantity yield [59]

$$d_n = (2.3 \pm 2.3) \times 10^{-25}\ \text{e-cm} \tag{3.130}$$

from which we infer

$$|d_n| \leq 5 \times 10^{-25}\ \text{e-cm} \tag{3.131}$$

In the quark model,

$$d_n = (4d_d - d_u)/3 \tag{3.132}$$

where d_d and d_u are the corresponding quark electric dipole moments. These receive contributions from the Higgs/quark diagrams of Fig. 16a, which are of order

$$d_q = \frac{O(1)}{16\pi^2} \frac{m_{q'}}{m_H^2} \mathrm{Im}(\lambda_1^* \lambda_3) \tag{3.133}$$

The O(1) factor in (3.133) covers a multitude of sins, including charge factors, $H\bar{H}$ mixing, and some tedious functions of m_H, m_q, and $m_{\tilde{q}}$. Taking $m_{q'} \approx 1$ GeV as a representative estimate, as well as our conventional $m_H \simeq 100$ GeV, when we compare (3.133) with the bound (3.93) we obtain entries (19,1) and (19,3) of the table. The corresponding D/quark diagrams of Figs. 16b yield an analogous estimate but with m_H^2 replaced by m_D^2 in the denominator. Since our conventional value of m_D is 300 GeV, this results in an upper bound on Im $\lambda_6\lambda_7$ which is nine times weaker, as shown in entries (19,4) and (19,5) of the table*). Finally, the D/lepton diagrams of Fig. 16c yield an estimate

*) This contribution to d_n is also studied in Ref. [60], which makes somewhat different assumptions about the masses of the particles in the loops.

analogous to (3.95) but with $m_{q'}/m_H^2$ replaced by m_ℓ/m_D^2 . Taking $m_\ell \approx 0.1$ GeV as a representative estimate, we arrive at the (19,6) and (19,7) entries in the table. There is no point in deriving and quoting the corresponding bound on Im $\lambda_9\lambda_{10}$ from the analogous D/neutrino diagrams, since it is much weaker than that obtained from the neutrino mass in subsection 2.3 and shown in entries (23,7) and (23,9) of the table.

3.6 Weak universality, etc.

3.6.1 $\pi \to e\nu$

The Standard Model predicts [57] that $R \equiv \Gamma(\pi^+ \to e^+\nu_e)/\Gamma(\pi^+ \to \mu^+\nu_\mu) = 1.233 \times 10^{-4}$ after including radiative corrections, whilst the experimental value [41] of R is $(1.228 \pm 0.22) \times 10^{-4}$, so

$$|\Delta R| = |(R_{exp} - R_{th})/R_{th}| < 0.022 \tag{3.134}$$

To calculate ΔR in a given theoretical framework, we parametrize [57] the relevant effective interactions as

$$\mathcal{L}_{eff}^{ee} = \frac{2G_F}{\sqrt{2}}\left[(\bar{d}\gamma^\mu\gamma_5 u)(\bar{\nu}_{e_L}\gamma_\mu e_L) + \bar{C}_{Pe}(\bar{d}\gamma^5 u)(\bar{\nu}_{e_L} e_R)\right] \tag{3.135}$$

and similarly with e replaced by μ. Parametrizing the ratio of hadronic matrix elements by

$$\frac{\langle 0|\bar{d}\gamma_\mu\gamma_5 u|\pi^+\rangle}{\langle 0|\bar{d}\gamma_5 u|\pi^+\rangle} = \frac{k_\mu}{m_\pi}\rho_P^{-1} \tag{3.136}$$

the theoretical prediction for ΔR [(3.134)] based on the effective interaction (3.135) is

$$\Delta R = \frac{1 + \frac{2m_\pi}{m_e}\rho_P \bar{C}_{Pe}}{1 + \frac{2m_\pi}{m_\mu}\rho_P \bar{C}_{P\mu}} \tag{3.137}$$

Since $m_\mu \gg m_e$, we drop the $\bar{C}_{P\mu}$ term in (3.137) and therefore use (3.134) and (3.137) to infer

$$\left|\frac{2m_\pi}{m_e}\rho_P \bar{C}_{Pe}\right| < 0.022 \tag{3.138}$$

Current algebra can be used to estimate

$$\rho_P = \frac{m_\pi}{m_u + m_d} \simeq 14 \tag{3.139}$$

which finally yields the bound

$$|\bar{C}_{Pe}| < 2.6 \times 10^{-6} \tag{3.140}$$

when inserted into the inequality (3.138).

The Higgs exchange diagram of Fig. 17a yields an effective interaction,

$$\mathcal{L}_{eff} = \frac{\lambda_2\lambda_5}{2m_H^2}\left[(\bar{d}u) - (\bar{d}\gamma_5 u)\right](\bar{e}_L e_R) \tag{3.141}$$

which after using (3.102) gives the bound shown in entries (20,2) and (20,3) of the table. There is no interesting limit from the D^c scalar exchange diagram of Fig. 17b, because it gives a $(V-A)$ form when Fierz-transformed, and so lacks the interesting enhancement (3.139) of the pseudoscalar contribution.

3.6.2 Quark/lepton universality

This is automatic in superstring models with $\langle 0|\tilde{\nu}^c|0\rangle \equiv y = 0$, as we advocate. If $y \neq 0$, the $\lambda_{10} D \nu^c d^c$ terms in the superpotential (2.1) will induce mixing between the d and D fields, as well as between the d^c and D^c fields. The corresponding leptonic mixing induced by the $HL\nu^c$ terms must be small, since their coefficients must be small in order to get small Dirac neutrino masses. Since the d is a member of a weak isodoublet, whilst the D is an isosinglet, their mixing could lead to a violation of weak universality*). To study the order of magnitude of this effect and to bound it using experimental data, we use the toy model of Section 2.6 with just one flavour each of d, d^c, D, and D^c. As was shown there [Eq. (2.23a)], the order of magnitude of mixing among d_L and D_L is

$$\theta_L \simeq \frac{\lambda_8 \lambda_{10} \bar{v} y}{(\lambda_8^2 x^2 + \lambda_{10}^2 y^2)} \tag{3.142}$$

which is an estimate of the expected violation of weak universality as measured by a breakdown of unitarity for the generalized Cabibbo–Kobayashi–Maskawa matrix,

$$1 = \sum_{i=d,s,b} (|V_{iu}|^2 + |V_{D_i u}|^2) \Rightarrow |V_{KM}|^2 \equiv \sum_{i=d,s,b} |V_{iu}|^2 < 1 \tag{3.143}$$

where

$$V_{D_i u} \sim \theta_L^i V_{iu} \quad ; \quad i = d,s,b \tag{3.144}$$

is a reasonable estimate.

A recent analysis [62] of the weak mixing angles has yielded

$$|V_{KM}|^2 = 0.9954 \pm 0.0025 \tag{3.145}$$

We believe that to be conservative, especially in view of the theoretical uncertainties in estimating U_{su}, the error quoted in (3.145) should be increased by a factor of 2, so that $U = 1$ is not excluded and a conservative bound is

$$|V_{KM}|^2 \geq 0.9904 \tag{3.146}$$

so that

$$\sum_i |V_{D_i u}|^2 \leq 0.0096 \tag{3.147}$$

---

*) This has also been studied in Ref. [61], with special attention to effects on the lifetime and decays of heavy quarks.

In the simplified case of one d and one D flavour, a bound such as (3.147) would correspond to

$$0.1 \gtrsim |\theta_L| = \frac{\lambda_3 \lambda_{10} \bar{v} y}{\lambda_5^2 x^2 + \lambda_{10}^2 y^2} \tag{3.148}$$

and hence

$$\lambda_5^2 x^2 + \lambda_{10}^2 y^2 \gtrsim 10 (\lambda_3 \lambda_{10} \bar{v} y) \tag{3.149}$$

In the realistic case of three generations, the bounds (3.148) and (3.149) apply to the mixing θ_L^d of the first d generation, whilst the corresponding bounds for the s and b generations would be relaxed by conventional Kobayashi-Maskawa angle factors:

$$(\lambda_5^2 x^2 + \lambda_{10}^2 y^2)_{d,s,b} \gtrsim \left(10, \frac{10}{s_1}, \frac{10}{s_1 s_3}\right)(\lambda_3 \lambda_{10} \bar{v} y)_{d,s,b} \tag{3.150}$$

In view of the known small values of λ_3(d, s, b), the constraints (3.150) impose no severe restrictions on the unknowns ($\bar{v}/x$, y/x, λ_6, λ_{10}), and so we leave row 21 of the table blank. Even if one arbitrarily assumes $\lambda_6 = \lambda_{10} = \lambda_3$, the best bound on x and y that one can obtain is

$$\left(\frac{x}{v}\right)^2 + \left(\frac{y}{v}\right)^2 \gtrsim 10\left(\frac{\bar{v}}{v}\right)\left(\frac{y}{v}\right) \sim (2 \text{ to } 3)\left(\frac{y}{v}\right) \tag{3.151}$$

where a dynamically preferred range of $\bar{v}/v$ has been inserted. This is compatible with $y/v \approx x/v$ and $x/v \gtrsim 3$ as required by other phenomenological constraints.

3.6.3 $\pi^0 \to e^+e^-$

This is not necessarily a test of weak universality, but we could not find a more appropriate place in our schema to present our results. Since the decay $\pi^0 \to e^+e^-$ may proceed via a $\gamma\gamma$ intermediate state as in Fig. 18a, so that the imaginary part of the $\pi^0 \to e^+e^-$ amplitude is related to the $\pi^0 \to \gamma\gamma$ rate, unitarity imposes a lower limit on the branching ratio $B^\pi = B(\pi^0 \to e^+e^-) \gtrsim B^\pi_{\text{unitarity}} = 4.75 \times 10^{-8}$. Now the experimental data on this branching ratio give [63, 64]

$$B^\pi_{exp} = (1.82 \pm 0.61) \times 10^{-7} = (3.8 \pm 1.3) B^\pi_{unitarity} \tag{3.152a}$$

$$B^\pi_{exp} = (2.26^{+2.43}_{-1.11}) \times 10^{-8} = (4.8^{+5.2}_{-2.4}) B^\pi_{unitarity} \tag{3.152b}$$

The real part of the $\pi^0 \to e^+e^-$ amplitude coming from the $\gamma\gamma$ intermediate state is, in general, model-dependent, but a recent theoretical analysis of different types of calculations finds [65] a total theoretical branching ratio

$$B^\pi_{TH} \simeq 1.3\, B^\pi_{unitarity} \simeq 6 \times 10^{-8} \tag{3.153}$$

well below the experimental branching ratio.

The difference between the experimental rate (3.152) and theoretical prediction (3.153) then corresponds to a branching ratio difference B^π_Δ:

$$B_D^\pi \simeq 1.2 \times 10^{-7} \tag{3.154a}$$

$$B_D^\pi \simeq 1.7 \times 10^{-7} \tag{3.154b}$$

Using the total decay width of the pion

$$\Gamma(\pi^0 \to \text{all}) = \frac{1}{\tau_{\pi^0}} = 8 \times 10^{-9}\,\text{GeV} \tag{3.155}$$

we may convert the branching ratio differences into decay width differences

$$\Gamma_\Delta^\pi \simeq 1.0 \times 10^{-15}\,\text{GeV} \tag{3.156a}$$

$$\Gamma_\Delta^\pi \simeq 1.3 \times 10^{-15}\,\text{GeV} \tag{3.156b}$$

We then bound possible new contributions to the $\pi^0 \to e^+e^-$ decay by demanding that they should not exceed the partial widths (3.156).

Figure 18b shows Higgs exchange contributions to this process, which give an effective interaction

$$\mathcal{L}_{\text{eff}} \simeq \frac{\lambda_2 \lambda_3}{m_H^2} (\bar{d}_R d_L)(\bar{e}_L e_R) \tag{3.157}$$

If the Higgs mass-mixing matrix includes ($H\bar{H}$) mixing of strength comparable to the diagonal mass terms there will also be an effective interaction (Fig. 18c)

$$\mathcal{L}_{\text{eff}} \simeq \frac{\lambda_1 \lambda_2}{m_H^2} (\bar{u}_R u_L)(\bar{e}_L e_R) \tag{3.158}$$

These effective interactions may induce a substantial decay rate owing to their lack of helicity suppression, and since there will be the matrix element enhancement ϱ_P for the pseudoscalar operator (3.139). So from the effective interaction (3.157) we obtain the decay width (with $f_\pi \approx 125$ MeV)

$$\begin{aligned} \Gamma(\pi^0 \to ee) &= \frac{(\varrho_P f_\pi)^2 m_\pi^3}{64\pi} \left(\frac{\lambda_1 \lambda_3}{m_H^2}\right)^2 \\ &= (4.1 \times 10^{-5}) \left(\frac{\lambda_1 \lambda_3}{m_H^2}\right)^2 \text{GeV} \end{aligned} \tag{3.159}$$

The requirement that this decay width should not exceed the decay width difference (3.156) then yields, for 100 GeV Higgs mass, the joint (21,1/2/3) entry of our table.

$\tilde{D}$ and $\tilde{D}^c$ exchange diagrams of Fig. 18d yield effective interactions of the form

$$\mathcal{L}_{\text{eff}} \simeq \frac{\lambda_8^2}{2m_{\tilde{D}^c}^2} (\bar{u}_L \gamma^\mu u_L)(\bar{e}_L \gamma_\mu e_L) + \frac{\lambda_9^2}{2m_{\tilde{D}}^2} (\bar{u}_R \gamma^\mu u_R)(\bar{e}_R \gamma_\mu e_R) \tag{3.160}$$

Owing to the helicity suppression of the matrix elements of these operators, we obtain no useful limits for the (21,6) and (21,7) entries of our table.

4. CONCLUDING REMARKS

In this paper we have investigated many constraints on phenomenological low-energy models inspired by the superstring. The constraints have included successes of the Standard Model such as $(g-2)_\mu$ and weak universality, flavour-changing neutral interactions, and the continued absence of novel interactions violating baryon or lepton number. After repeating previous arguments disfavouring other compactification manifolds and gauge groups, we have studied models based on the $SU(3)_c \times SU(2)_L \times U(1)^{2or3}$ gauge groups suggested by Calabi–Yau compactification. After repeating previous arguments against an intermediate mass scale in such models, we have presented a new one based on an analysis of the charge $-1/3$ quark mass matrix.

We have analysed in some detail the problem of proton decay in superstring-inspired models. Dimension-four baryon-number-violating superpotential terms must be forbidden in order to avoid renormalizable proton decay interactions, and dimension-six operators do not induce proton decay at an observable rate owing to the elevated unification mass. In models with light fields from the **27** only, there are no gauge-invariant baryon-number-violating dimension-five operators, and so the proton will *not* decay at an experimentally accessible rate. Although it might be possible to avoid this conclusion by the *ad hoc* introduction of fields from split $\mathbf{27} + \overline{\mathbf{27}}$ multiplets, combined with new light singlet fields and specially arranged $\overline{\mathbf{27}}\ \mathbf{27}\ \mathbf{1}$ superpotential couplings, none the less it remains the case that the *non-observation* of proton decay at observable rates is a basic prediction of these superstring-inspired models.

Neutrino masses, either from tree-level couplings or from radiative corrections, were analysed. In order that the tree-level mass induced by the superpotential term $\lambda_0 HL\nu^c$ be less than the cosmological bound of 25 eV, we have seen that $\lambda_0 \lesssim 10^{-9}$ is necessary. The $\lambda_{10} D\nu^c d^c$ superpotential coupling, when combined with $\lambda_9 D^c LQ$ or $\lambda_8 D\ell^c u^c$, was able to generate Dirac neutrino mass terms at the one- or two-loop level, respectively. These satisfied the cosmological bound, for reasonable values of the other parameters, provided $\lambda_9\lambda_{10} \lesssim 10^{-6}$, and without significant restriction on the λ_8 coupling. We wish to emphasize that all neutrino masses coming from these tree or loop processes are Dirac masses, and that they conserve lepton number. In the absence of any effective mechanism for generating lepton-number-violating Majorana masses in these models, we expect lepton-number-violating processes such as neutrinoless double β decay, and $\nu \leftrightarrow \bar{\nu}$ oscillations to be absent. So the absence of lepton-number-violating effects from possible neutrino masses is another basic prediction of these superstring-inspired models. It is possible for discrete symmetries of the low-energy superpotential to arise in Calabi–Yau compactifications of superstrings. We give explicit examples of simple discrete symmetries which, if they arose in the compactification, would suffice to naturally avoid the unseen phenomena of proton decay and neutrino masses.

The most substantial part of our paper has been the derivation of bounds on Yukawa superpotential couplings obtained from various flavour-changing neutral interaction processes and from precision tests of Standard Model predictions*). The resulting bounds on the Yukawa couplings

---

*) See also Ref. [66] for a recent discussion of flavour-changing interactions mediated by scalar leptoquarks.

are compiled in the table. Shown at the bottom of each column are the best bounds on the real and imaginary parts of the couplings, and the processes from which they were derived. None of these bounds are significantly smaller than the known Yukawa couplings responsible for quark and lepton masses, so superstring models survive the challenges made by these processes. However, fresh theoretical interest in these rare processes and precision tests appears, because future experimental probes of them might well reveal discrepancies with the Standard Model which could be circumstantial evidence for some superstring model. We now go through each column in turn and identify the best experimental probes for superstring effects.

In column 1 we see that the $\lambda_1 HQu^c$ coupling is most severely constrained by the absence of D^0–$\bar{D}^0$ mixing, whilst other rare D decays are not competitive. One should push the upper limit on D^0–$\bar{D}^0$ mixing down to the range expected in the Standard Model. In column 2 we see that looking for $\mu \to e\gamma$ and for $\mu \to e\bar{e}e$ decay is the best way to probe the $\lambda_2 \bar{H}Le^c$ coupling. The best limit on the $\lambda_3 \bar{H}Qd^c$ coupling in column 3 comes from K^0–$\bar{K}^0$ mixing, whilst the present upper limit on B^0–$\bar{B}^0$ mixing is quite competitive and should be significantly improved. Several processes ($K_L \to \mu^+\mu^-$, $K_L \to \mu^\pm e^\mp$, $\mu N \to eN$, $\pi^+ \to e^+\nu$) give comparable limits on the product $\lambda_2\lambda_3$. Currently, they are not as good as the products of the individual limits on the couplings λ_2 and λ_3, but the experimental limits on $K_L \to \mu^\pm e^\mp$, $\mu N \to eN$, and $\pi^+ \to e^+\nu$ could be improved to become highly competitive. Column 3 also shows that the best limit on Im λ_3 is provided by CP violation in the K^0–$\bar{K}^0$ mass matrix, which is unlikely to improve in the near future. Columns 4 and 5 indicate that the upper limits on D^0–$\bar{D}^0$, B^0–$\bar{B}^0$ mixing and on Re (K^0–$\bar{K}^0$) provide the best bounds on the $\lambda_6 \bar{D}QQ$, $\lambda_7 D^c u^c d^c$ couplings—another reason to improve these measurements. The imaginary parts of λ_6 and λ_7 are most severely constrained by CP violation in the K^0–$\bar{K}^0$ system, and by the neutron electric dipole moment, which would be exceedingly interesting to measure more accurately. We see in columns 6 and 7 that the best limit on the $\lambda_8 D\ell^c u^c$ and $\lambda_9 D^c LQ$ couplings is provided by the experimental limit on $\mu N \to eN$, which could well be improved in the future. Column 8 shows that there is no very good limit on the $\lambda_{10} Dd^c\nu^c$ coupling if $\langle 0|\tilde{\nu}^c|0\rangle = 0$, whilst columns 9 and 10 show that several processes ($K_L \to \mu^+\mu^-$, K^0–$\bar{K}^0$, B^0–$\bar{B}^0$) impose comparable limits of order 10^{-2} on the d/D mixing angles if $\langle 0|\tilde{\nu}^c|0\rangle \neq 0$. We will return later to the implications of this result for model-building. We see also in column 8 that the neutron electric dipole moment and CP violation in the (K^0–$\bar{K}^0$) system again impose the most stringent upper limits on Im λ_{10}.

Thus the processes whose improved measurement would be the most interesting from the point of view of the superstring models discussed here are D^0–$\bar{D}^0$ mixing, $\mu \to e\gamma$, $\mu \to e\bar{e}e$, B^0–$\bar{B}^0$, $\mu N \to eN$, and the neutron electric dipole moment. If the Standard Model prediction for one of these processes were found to fail, some superstring model could be the culprit. On the other hand, the least interesting from this limited perspective seem to be $K^+ \to \pi^+e^+e^-$, $K^+ \to \pi^+\mu^\pm e^\mp$, rare D decays, $(g-2)_\mu$, ϵ'/ϵ, P($K \to \pi\mu\nu$), $\pi^0 \to e^+e^-$, and Cabibbo–Kobayashi–Maskawa universality. If the Standard Model were soon to be invalidated by modest improvements in measurements of these processes, the superstring would not be a likely culprit.

Finally, we turn to the implications for model-building of the bottom lines of columns 9 and 10. As discussed in Section 2, generating $\langle 0|\tilde{\nu}^c|0\rangle \neq 0$ requires driving $m^2_{\tilde{\nu}^c} < 0$ using Yukawa couplings in

the renormalization group equations. In view of the experimental and cosmological upper limits on neutrino masses, the $\lambda_4 HL\nu^c$ coupling cannot be large enough to drive $m^2_{\tilde{\nu}^c} < 0$, and the only remaining candidate is $\lambda_{10} Dd^c\nu^c$. However, in view of the upper limits in columns 9 and 10, particularly those from the absence of B^0-$\overline{B}^0$ mixing, it seems unlikely that any λ_{10} coupling is large enough ($|\lambda_{10}| \gtrsim 0.2$) to drive $m^2_{\tilde{\nu}^c} < 0$. Therefore it seems difficult to construct dynamical models with $\langle 0|\tilde{\nu}^c|0\rangle \neq 0$ which are phenomenologically viable. This means, in particular, that the four-dimensional gauge group obtained after compactification should have rank 5.

The tabulated limits assume that couplings are roughly independent of generation. However, it is easy to see, by reference to the explicit calculations reported in the text, which generation-dependent couplings are the most severely constrained in each case. This would enable us to confront our bounds with specific models (such as in Ref. [37]) with generation-dependent zeros in the tree-level superpotential.

We conclude with a consumer advisory warning: No one knows how to compactify the superstring. Calabi–Yau compactification could be wrong, in which case many of the arguments in this paper would be irrelevant. Even if Calabi–Yau compactification, or something similar, is correct, many of the arguments in this paper are not watertight and could undoubtedly be evaded. Nevertheless, we believe that the analysis presented here adds interest to experimental studies of rare processes and precision tests of the Standard Model, and could even tell us something useful about superstring phenomenology.

Acknowledgements

The hospitality extended to three of us (B.A.C., K.E., and M.K.G.) by the CERN Theory Division and to two of us (B.A.C. and J.E.) by the Lake Louise Winter Institute is warmly acknowledged. The research of B.A.C. is supported in part by NSERC grant A 8863; he thanks Luis Ibáñez for many helpful discussions. The research of K.E. and D.V.N. was supported in part by DOE grant DE-AC02-76ER0081 and in part by the University of Wisconsin Research Committee with funds granted by the Wisconsin Alumni Research Foundation. The research of M.K.G. is supported in part by the US Department of Energy under contract DE-AC03-76SF00098 and in part by the National Science Foundation under grant number PHY-85-15857.

REFERENCES

[1] For a review see: J. Schwarz, Superstrings—the first 15 years (World Scientific Publishing Company, Singapore, 1985).

[2] For a review see: J. Ellis, CERN preprint TH.4439/86 (1986), presented at the Seventh Workshop on Grand Unification, ICOBAN '86.

[3] For a review see: P. Langacker, Phys. Rep. **72C** (1981) 185.

[4] For a review see: L.B. Okun, Leptons and quarks (North-Holland Publ. Co., Amsterdam, 1982).

[5] For a review see: E. Farhi and L. Susskind, Phys. Rep. **74C** (1981) 277.

[6] For reviews see:
H.P. Nilles, Phys. Rep. **110C** (1984) 1.
H. Haber and G.L. Kane, Phys. Rep. **117C** (1985) 75.

[7] P. Candelas, G. Horowitz, A. Strominger and E. Witten, Nucl. Phys. **B258** (1985) 46.

[8] E. Calabi, Algebraic geometry and topology, a Symposium in Honour of S. Lefschetz (Princeton University Press, Princeton, NJ, 1951).
S.-T. Yau, Proc. Nat. Acad. Sci. **74** (1977) 1798.

[9] M.T. Grisaru, A. van der Ven and D. Zanon, Phys. Lett. **178B** (1986) 423; Nucl Phys. **B277** (1986) 388 and 409.
D.J. Gross and E. Witten, Princeton Univ. preprint (1986).
M.D. Freeman and C.N. Pope, Imperial College preprint TP/85-86/17 (1986).
D. Nemeschansky and A. Sen, Phys. Lett. **178B** (1986) 365.
A. Sen, Phys. Lett. **178B** (1986) 370.

[10] E. Witten, Nucl. Phys. **B268** (1986) 79.

[11] C. Hull, Phys. Lett. **178B** (1986) 357.
A. Strominger, ITP preprint NSF-ITP-86-16 (1986).

[12] J. Ellis, C. Gómez, D.V. Nanopoulos and M. Quirós, Phys. Lett. **173B** (1986) 59.

[13] M. Dine, N. Seiberg, X.-G. Wen and E. Witten, Nucl. Phys. **B278** (1986) 769.

[14] J. Ellis, K. Enqvist, D.V. Nanopoulos, K. Olive, M. Quirós and F. Zwirner, Phys. Lett. **176B** (1986) 403.

[15] L. Dixon, J. Harvey, C. Vafa and E. Witten, Nucl. Phys. **B261** (1985) 678 and **B274** (1986) 285.

[16] Y. Hosotani, Phys. Lett. **129B** (1985) 193.

[17] E. Witten, Nucl. Phys. **B258** (1985) 75.

[18] S. Cecotti, J.-P. Derendinger, S. Ferrara, L. Girardello and M. Roncadelli, Phys. Lett. **156B** (1985) 31.
J.D. Breit, B.A. Ovrut and G. Segré, Phys. Lett. **158B** (1985) 33.
A. Sen, Phys. Rev. Lett. **55** (1985) 33.
M. Dine, V. Kaplunovsky, M. Mangano, C. Nappi and N. Seiberg, Nucl. Phys. **B259** (1985) 519.

[19] A. Strominger and E. Witten, Commun. Math. Phys. **101** (1985) 341.
A. Strominger, Phys. Rev. Lett. **55** (1985) 2547.

[20] H. Georgi and D.V. Nanopoulos, Phys. Lett. **82B** (1979) 95.

[21] S.L. Glashow and S. Weinberg, Phys. Rev. **D15** (1977) 1958.
M.S. Chanowitz, J. Ellis and M.K. Gaillard, Nucl. Phys. **B128** (1979) 506.

[22] J. Ellis and D.V. Nanopoulos, Phys. Lett. **110B** (1982) 44.
T. Inami and C.S. Lim, Nucl. Phys. **B207** (1982) 533.
B. Campbell, Phys. Rev. **D28** (1983) 209.
G.K. Leontaris, K. Tamvakis and J.D. Vergados, Phys. Lett. **171B** (1986) 412 and references therein.

[23] J. Ellis, K. Enqvist, D.V. Nanopoulos and F. Zwirner, Nucl. Phys. **B276** (1986) 14.

[24] B. Campbell, J. Ellis, M.K. Gaillard, D.V. Nanopoulos and K.A. Olive, Phys. Lett. **180B** (1986) 77.
J. Ellis, K. Enqvist, D.V. Nanopoulos and K. Olive, preprint CERN-TH.4613/86 (1986).

[25] G.F. Chapline and N. Manton, Phys. Lett. **120B** (1983) 105.
A.H. Chamseddine, Nucl. Phys. **B185** (1981) 403.
E. Bergshoeff, M. de Roo, B. de Wit and P. van Nieuwenhuizen, Nucl. Phys. **B195** (1982) 97.

[26] K. Yamamoto, Phys. Lett. **168B** (1986) 341.
K. Enqvist, D.V. Nanopoulos and M. Quirós, Phys. Lett. **169B** (1986) 343.

[27] J. Ellis, K. Enqvist, D.V. Nanopoulos and K. Olive, CERN preprint TH.4613/86 (1986).

[28] E. Cremmer, S. Ferrara, C. Kounnas and D.V. Nanopoulos, Phys. Lett. **133B** (1983) 61.

[29] J. Ellis, A.B. Lahanas, D.V. Nanopoulos and K. Tamvakis, Phys. Lett. **134B** (1984) 429.
J. Ellis, C. Kounnas and D.V. Nanopoulos, Nucl. Phys. **B241** (1984) 406.
For a review see: A.B. Lahanas and D.V. Nanopoulos, Phys. Rep. **145C** (1987) 1.

[30] N. Sakai and T. Yanagida, Nucl. Phys. **B197** (1982) 533.
S. Weinberg, Phys. Rev. **D26** (1982) 187.

[31] S. Sarkar and A.M. Cooper, Phys. Lett. **148B** (1984) 347.

[32] A. Masiero, D.V. Nanopoulos and A. Sanda, Phys. Rev. Lett. **57** (1986) 663.

[33] V.A. Lubimov et al., Proc. 22nd Int. Conf. on High-Energy Physics, Leipzig, 1984, eds. A. Meyer and E. Wieczorek (Akad. der Wiss. der DDR, Zeuthen, 1984), Vol. II, p. 108.

[34] S.P. Mikheyev and A.Yu. Smirnov, *in* Proc. 10th Int. Workshop on Weak Interactions, Savonlinna, Finland, 1985.
H.A. Bethe, Phys. Rev. Lett. **56** (1986) 1305.

[35] K. Enqvist and J. Maalampi, Phys. Lett. **180B** (1986) 347.

[36] See, for instance: A. Vilenkin, Phys. Rep. **121** (1985) 263.

[37] B.R. Greene, K.H. Kirklin, P. Miron and G.G. Ross, Phys. Lett. **180B** (1986) 69 and Nucl. Phys. **B238** (1986) 667.

[38] M.-K. Gaillard and B.W. Lee, Phys. Rev. **D10** (1974) 897.

[39] For reviews see:
L.L. Chau, Phys. Rep. **95** (1983) 3.
P. Langacker, Proc. First Aspen Winter Physics Conf., Aspen (Colo.), 1985, ed. M.M. Block (N.Y. Acad. Sci., New York, 1986), p. 725.

[40] G. Beal, M. Bander and A. Soni, Phys. Rev. Lett. **48** (1982) 848.
I. Bigi and J.-M. Frère, Phys. Lett. **129B** (1983) 469.
[41] Particle Data Group, M. Aguilar-Benitez et al., Phys. Lett. **170B** (1986) 1.
[42] D. Bryman, *in* New Frontiers in Particle Physics, Proc. First Lake Louise Winter Institute, eds. J.M. Cameron et al. (World Scientific, Singapore, 1986), p. 353.
[43] W.C. Louis et al., Phys. Rev. Lett. **56** (1986) 1027.
[44] MARK II Collaboration, K. Riles et al., Stanford preprint SLAC-PUB-4156 (1986);
ACCMOR Collaboration, H. Palka et al., preprint CERN EP/87-10 (1987).
[45] MARK III Collaboration, J.J. Becker et al., Stanford preprint, SLAC-PUB-4194 (1987).
[46] CLEO Collaboration, R. Poling, Talk presented at the XXIII Int. Conf. on High Energy Physics, Berkeley, Univ. of Rochester preprint UR-971 (1986).
[47] CLEO Collaboration, P. Avery et al., Phys. Lett. **183B** (1987) 429.
[48] D. Bryman et al., Phys. Rev. Lett. **55**, 465 (1985);
D. Bryman, TRIUMF preprint TRI-PP-86-83 (1986).
[49] H.K. Walter et al., Nucl. Phys. **A434** (1985) 409.
[50] O. Shanker, Nucl. Phys. **B206** (1982) 253.
[51] R.D. Bolton et al., Phys. Rev. Lett. **56** (1986) 2461.
[52] J.A. Grifols and A. Méndez, Phys. Rev. **D26** (1982) 1809.
J. Ellis, J. Hagelin and D.V. Nanopoulos, Phys. Lett. **116B** (1982) 283.
R. Barbieri and L. Maiani, Phys. Lett. **117B** (1982) 203.
T.-C. Yuan, R. Arnowitt, A.H. Chamseddine and P. Nath, Z. Phys. **C26** (1984) 407.
[53] R.C. Larsen et al., Phys. Rev. Lett. **54** (1985) 1628.
[54] R. Bernstein et al., Phys. Rev. Lett. **54** (1985) 1631.
[55] S. Weinberg, Phys. Rev. Lett. **37** (1976) 657.
[56] J.F. Donoghue and B.R. Holstein, Phys. Rev. **D32** (1985) 1152.
[57] O. Shanker, Nucl. Phys. **B204** (1982) 375.
[58] M.P. Schmidt et al., Phys. Rev. Lett. **43** (1979) 556.
[59] I.S. Altarev et al., Phys. Lett. **102B** (1981) 13.
[60] A. Barroso and J. Maalampi, CERN preprint TH.4550/86 (1986).
[61] K. Enqvist, J. Maalampi and M. Roos, Phys. Lett. **176B** (1986) 396.
[62] W.J. Marciano and A. Sirlin, Phys. Rev. Lett. **56** (1986) 22.
[63] R.E. Mishke et al., Phys. Rev. Lett. **48** (1982) 1153.
[64] J. Fischer et al., Phys. Lett. **73B** (1978) 364 and **76B** (1978) 663 (E).
[65] L. Bergstrom et al., Phys. Lett. **126B** (1983) 117.
[66] W. Buchmüller and D. Wyler, Phys. Lett. **177B** (1986) 377.

Bounds on Yukawa couplings from flavour-changing neutral currents and other rare processes.
The generation structure of the couplings has not been taken explicitly into account, but it is clear, for each process studied, which fermion generations are involved.

	Rare process		Superpotential term									
			1	2	3	4	5	6	7	8	9	10
			$\lambda_1 HQu^c$	$\lambda_2 \bar{H}Le^c$	$\lambda_3 \bar{H}Qd^c$	$\lambda_6 DQQ$	$\lambda_7 D^c u^c d^c$	$\lambda_8 D\ell^c u^c$	$\lambda_9 D^c LQ$	$\lambda_{10} Dd^c \nu^c$ $\langle 0\|\tilde{\nu}^c\|0\rangle = 0$	ϵ_L $\langle 0\|\tilde{\nu}^c\|0\rangle \neq 0$	ϵ_R $\langle 0\|\tilde{\nu}^c\|0\rangle \neq 0$
K physics	1	$K^0 \leftrightarrow \bar{K}^0$	–	–	3×10^{-5}	0.1	0.1	–	0.1	0.1	1×10^{-2}	3×10^{-2}
	2	$K_L \to \mu^+\mu^-$	–	$\sqrt{\lambda_3\lambda_2} < 8 \times 10^{-4}$		0.4	0.4	–	0.6	0.2	6×10^{-3}	3×10^{-2}
	3	$K \to \pi\bar{\nu}\nu$	–	–		–	–	–	0.2	0.2	2×10^{-2}	0.1
	4	$K \to \pi e^+ e^-$	–	$\sqrt{\lambda_3\lambda_2} < 8 \times 10^{-3}$		0.9	0.9	–	–	–	–	–
	5	$K_L \to \mu^\pm e^\mp$	–	$\sqrt{\lambda_3\lambda_2} < 6 \times 10^{-4}$		–	–	–	–	–	–	–
	6	$K^+ \to \pi^+\mu^\pm e^\mp$	–	$\sqrt{\lambda_3\lambda_2} < 2 \times 10^{-3}$		–	–	–	–	–	–	–
D physics	7	$D^0 \leftrightarrow \bar{D}^0$	2×10^{-4}	–	–	0.1	0.1	0.1	0.1	–	–	–
	8	$D^0 \to \mu^+\mu^-$	$\sqrt{\lambda_1\lambda_2} < 6 \times 10^{-2}$		–	–	–	–	–	–	–	–
	9	$D^0 \to \mu^\pm e^\mp$	$\sqrt{\lambda_1\lambda_2} < 6 \times 10^{-2}$		–	–	–	2	2	–	–	–
	10	$D \to \mu^\pm e^\mp X$	$\sqrt{\lambda_1\lambda_2} < 0.2?$		–	–	–	1.?	1.?	–	–	–
B physics	11	$B^0 \leftrightarrow \bar{B}^0$	–	–	1×10^{-4}	0.1	0.1	–	0.1	0.1	1×10^{-2}	3×10^{-2}
μ physics	12	$\mu N \to eN$	–	$\sqrt{\lambda_3\lambda_2} < 8 \times 10^{-4}$		–	–	4×10^{-3}	4×10^{-3}	–	–	–
	13	$\mu \to \bar{e}ee$	–	2×10^{-3}	–	–	–	0.02	0.02	–	–	–
	14	$\mu \to e\gamma$	–	8×10^{-4}	–	–	–	0.1	0.1	–	–	–
	15	$(g-2)_\mu$	–	–	–	–	–	–	–	–	–	–

Rare process			Superpotential term									
			1	2	3	4	5	6	7	8	9	10
			$\lambda_1 HQu^c$	$\lambda_2 \bar{H}Le^c$	$\lambda_3 \bar{H}Qd^c$	$\lambda_6 DQQ$	$\lambda_7 D^c u^c d^c$	$\lambda_8 D\ell^c u^c$	$\lambda_9 D^c LQ$	$\lambda_{10} Dd^c \nu^c$ $\langle 0\|\tilde{\nu}^c\|0\rangle = 0$	ϵ_L $\langle 0\|\nu^c\|0\rangle \neq 0$	ϵ_R $\langle 0\|\nu^c\|0\rangle \neq 0$
CP violation (Im λ)	16	$\mathrm{Im}\,(K^0 \leftrightarrow \bar{K}^0)$	–	–	1×10^{-6}	2×10^{-2}	2×10^{-2}	–	2×10^{-2}	2×10^{-2}	2×10^{-3}	5×10^{-3}
	17	ϵ'/ϵ	–	–	–	–	–	–	–	–	–	–
	18	$P(K \to \pi\mu\nu)$	–	$\sqrt{\lambda_3\lambda_2} < 6 \times 10^{-3}$		–	–	–	–	–	–	–
	19	d_n	$\sqrt{\mathrm{Im}\,\lambda_1\lambda_3} < 6 \times 10^{-3}$	–	$\sqrt{\mathrm{Im}\,\lambda_1\lambda_3} < 6 \times 10^{-3}$	$\sqrt{\mathrm{Im}\,\lambda_6\lambda_7} < 2 \times 10^{-2}$		$\sqrt{\mathrm{Im}\,\lambda_8\lambda_9} < 6 \times 10^{-2}$		2×10^{-2}	–	–
Weak universality	20	$\pi \to e\nu$	–	$\sqrt{\lambda_3\lambda_2} < 1 \times 10^{-3}$		–	–	–	–	–	–	–
	21	$\pi^0 \to ee$		$\sqrt{\lambda_{1,3}\lambda_2} < 0.2$		–	–	–	–	–	–	–
	22	U_{KM}	–	–	–	–	–	–	–	–	–	–
ν mass	23	m_ν	–	–	–	–	–	–	$\sqrt{\lambda_9\lambda_{10}} < 1 \times 10^{-3}$			
Best limit (process)		Re λ	2×10^{-4} $D^0 \leftrightarrow \bar{D}^0$	8×10^{-4} $\mu \to e\gamma$	3×10^{-5} $\mathrm{Re}\,(K^0 \leftrightarrow \bar{K}^0)$	0.1 $\mathrm{Re}\,(K^0\text{-}\bar{K}^0)$ $\mathrm{Re}\,(D^0\text{-}\bar{D}^0)$ $\mathrm{Re}\,(B^0\text{-}\bar{B}^0)$	0.1 $\mathrm{Re}\,(K^0\text{-}\bar{K}^0)$ $\mathrm{Re}\,(D^0\text{-}\bar{D}^0)$ $\mathrm{Re}\,(B^0\text{-}\bar{B}^0)$	4×10^{-3} $\mu N \to eN$	4×10^{-3} $\mu N \to eN$	0.1 $K^0 \leftrightarrow \bar{K}^0$ $B^0 \leftrightarrow \bar{B}^0$	2×10^{-3} $\mathrm{Im}\,(K^0\text{-}\bar{K}^0)$	5×10^{-3} $\mathrm{Im}\,(K^0\text{-}\bar{K}^0)$
		Im λ	2×10^{-4} $D^0 \leftrightarrow \bar{D}^0$	8×10^{-4} $\mu \to e\gamma$	1×10^{-6} $\mathrm{Im}\,(K^0 \leftrightarrow \bar{K}^0)$	2×10^{-2} $\mathrm{Im}\,(K^0\text{-}\bar{K}^0)$	2×10^{-2} $\mathrm{Im}\,(K^0\text{-}\bar{K}^0)$	4×10^{-3} $\mu N \to eN$	4×10^{-3} $\mu N \to eN$	2×10^{-2} $\mathrm{Im}\,(K^0\text{-}\bar{K}^0)$ d_n		

Figure captions

Fig. 1 : Possible mechanism for baryon decay in a superstring model with a light singlet ϕ as well as quarks and leptons in the fundamental **27** of E_6.

Fig. 2 : Loop diagrams capable of generating Dirac neutrino masses: (a), (b) at the one-loop level, (c), (d) at the two-loop level.

Fig. 3 : One-loop diagrams which might contribute to $\nu' \to \nu + \gamma$ decay.

Fig. 4 : Possible contributions to $(\bar{s}d)^2$ operators relevant to K^0–$\bar{K}^0$ mixing.

Fig. 5 : Possible contributions to $K^0 \to \mu^+\mu^-, e^+e^-$ decays.

Fig. 6 : Possible contributions to $(\bar{s}d)(\bar{\nu}\nu)$ operators relevant to $K^+ \to \pi^+\bar{\nu}\nu$ decay.

Fig. 7 : Possible contribution to $K^0 \to \mu^{\mp}e^{\pm}$ decay.

Fig. 8 : Possible contributions to $(\bar{c}u)^2$ operators relevant to D^0–$\bar{D}^0$ mixing.

Fig. 9 : Possible contributions to $D^0 \to \mu^{\mp}e^{\pm}$ decay.

Fig. 10 : Possible contributions to anomalous $\mu N \to eN$ conversion.

Fig. 11 : Possible contributions to $\mu \to e\bar{e}e$ decay.

Fig. 12 : Possible contributions to $\mu \to e\gamma$ decay.

Fig. 13 : Possible contributions to the anomalous magnetic moment of the muon $(g-2)_\mu$.

Fig. 14 : Possible contributions to $\Delta I = 1/2$ K decays.

Fig. 15 : Possible contributions to muon polarization in $K \to \pi\mu\nu$ decay.

Fig. 16 : Possible contributions to the neutron electric dipole moment d_n.

Fig. 17 : Diagrams which could violate $(\mu - e)$ universality in $\pi^{\pm}$ decay.

Fig. 18 : Possible contributions to $\pi^0 \to e^+e^-$ decay.

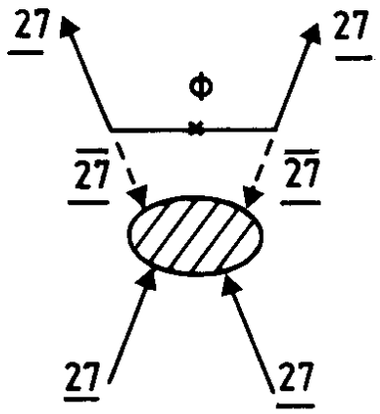

Fig. 1

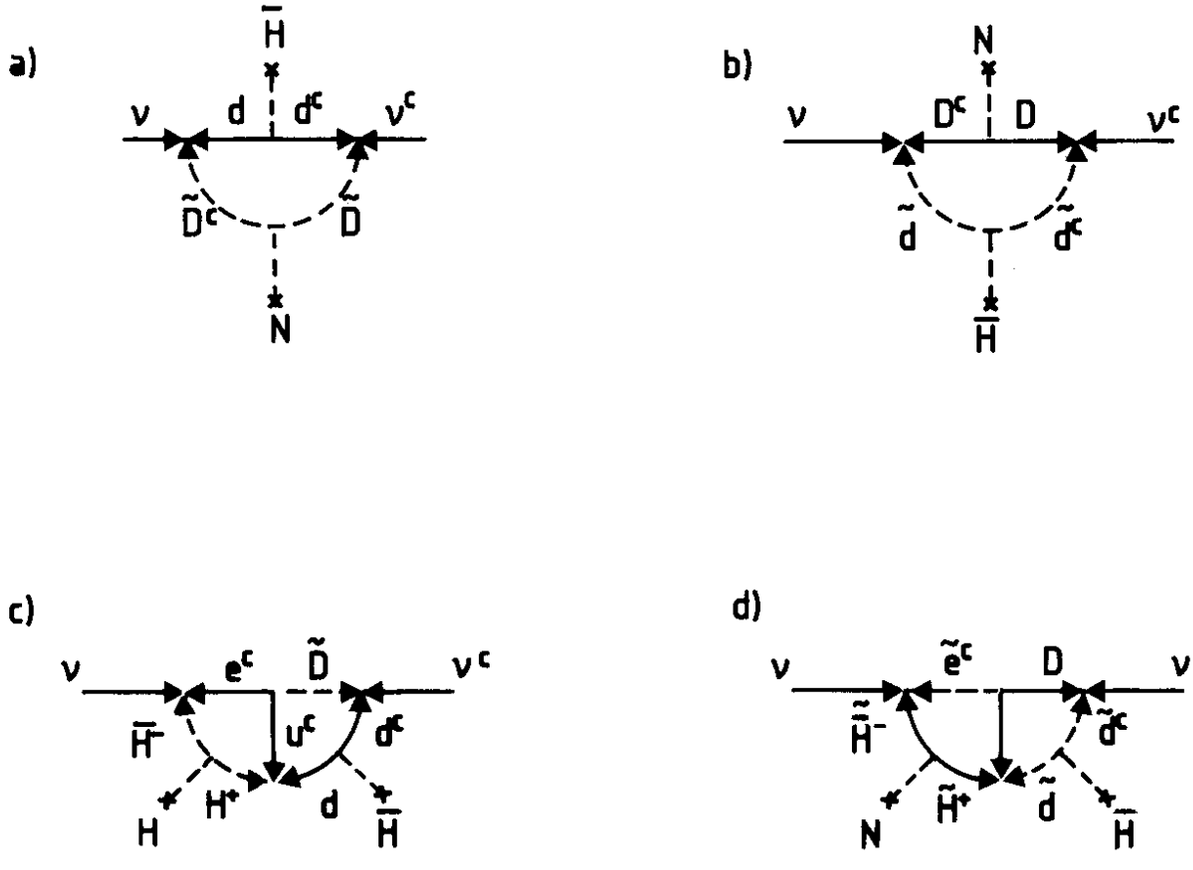

Fig. 2

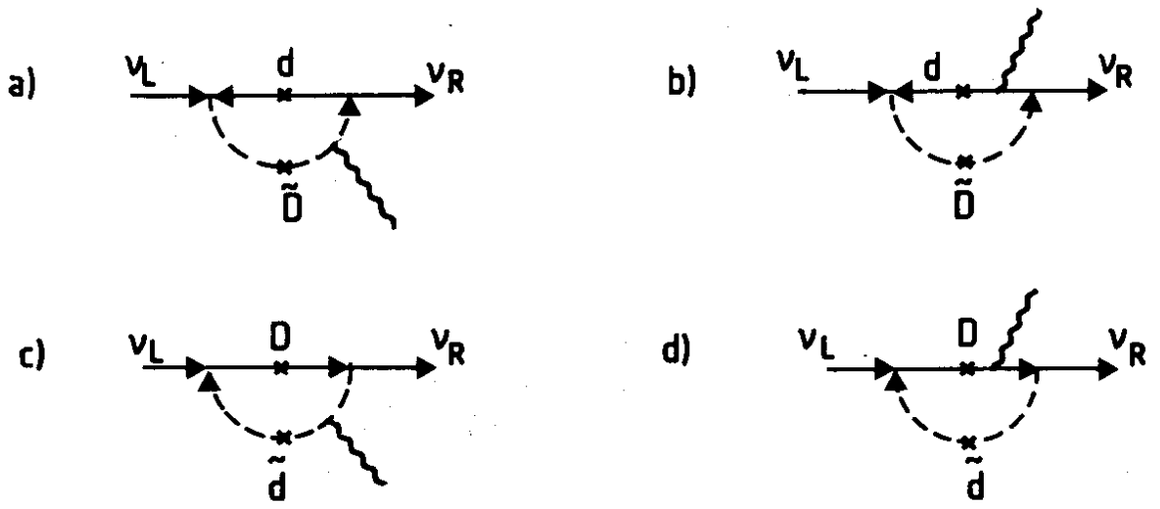
a)
ν_L
d
ν_R
$\tilde{D}$
b)
ν_L
d
ν_R
$\tilde{D}$
c)
ν_L
D
ν_R
$\tilde{d}$
d)
ν_L
D
ν_R
$\tilde{d}$

Fig. 3

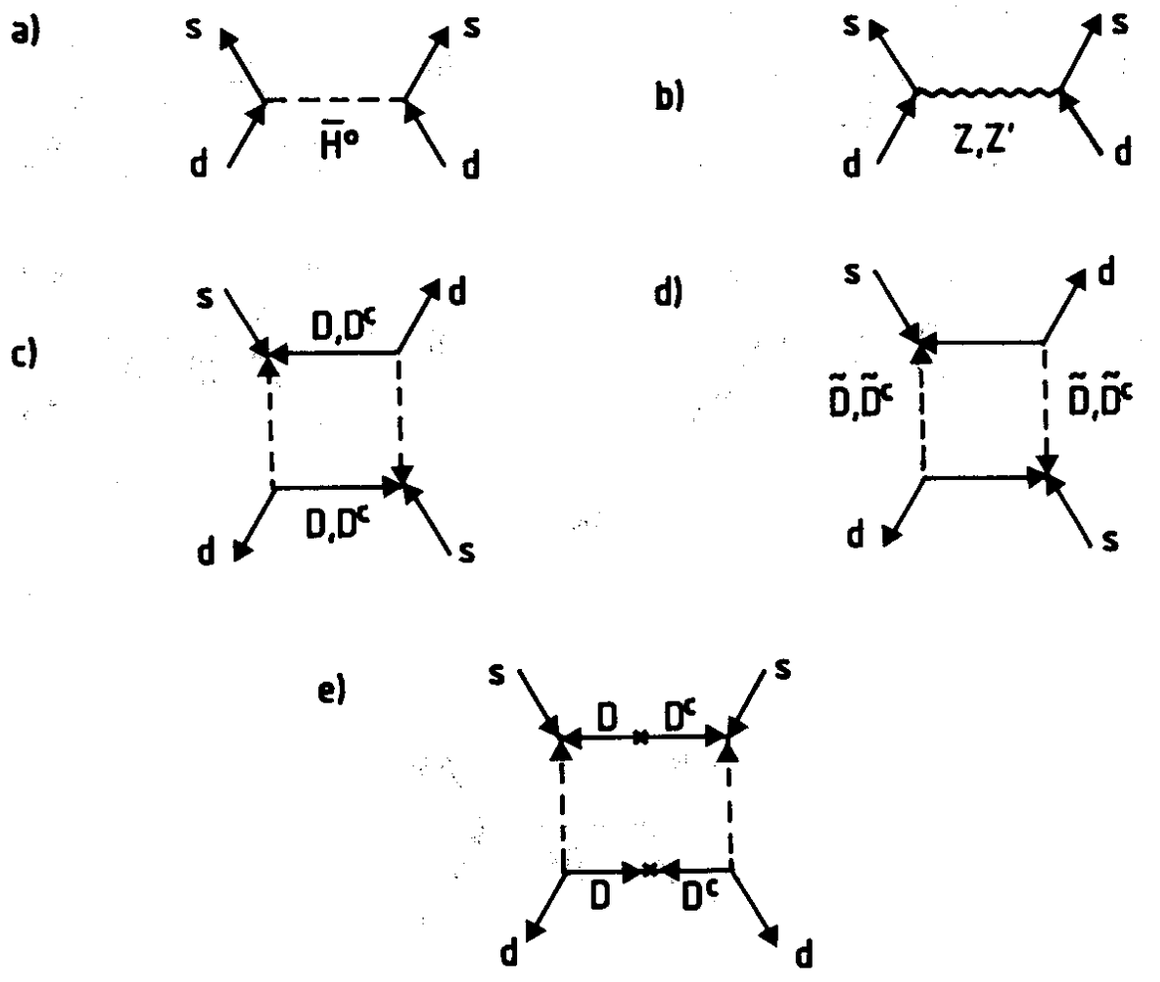
a)
s
s
d
$\bar{H}^o$
d
b)
s
s
d
Z,Z'
d
c)
s
d
D,D^c
d
D,D^c
s
d)
s
d
$\tilde{D}$,$\tilde{D}^c$
$\tilde{D}$,$\tilde{D}^c$
d
s
e)
s
s
D
D^c
D
D^c
d
d

Fig. 4

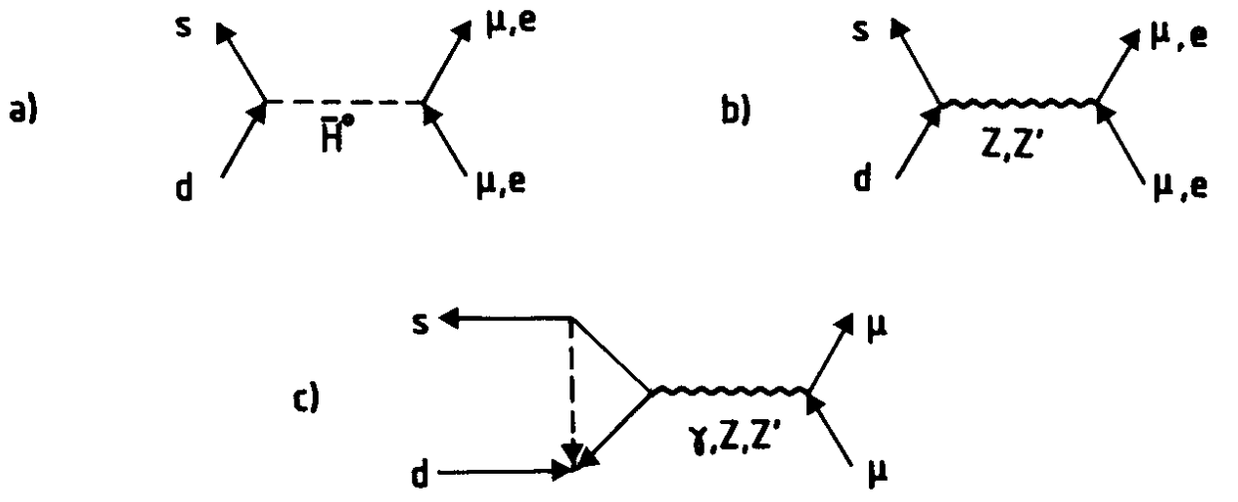

Fig. 5

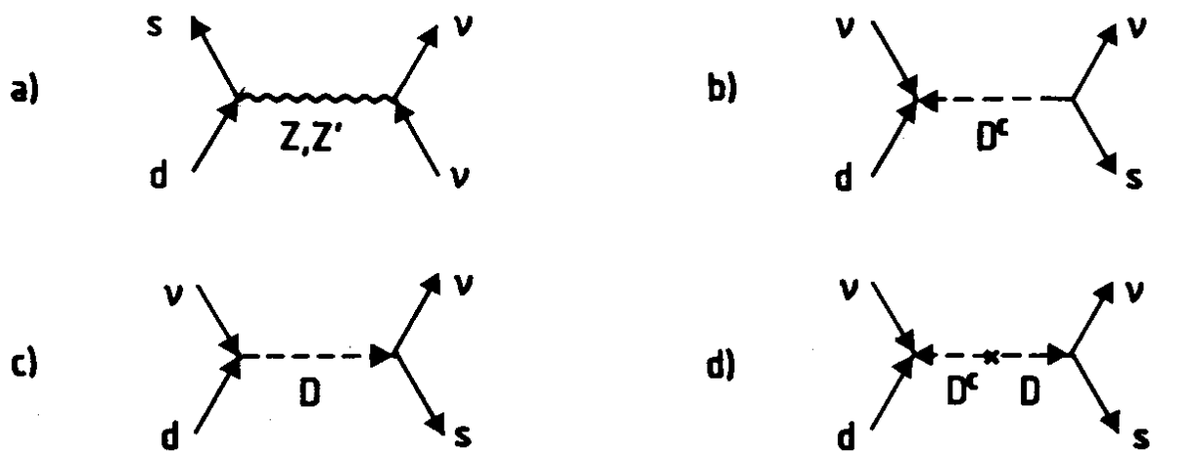

Fig. 6

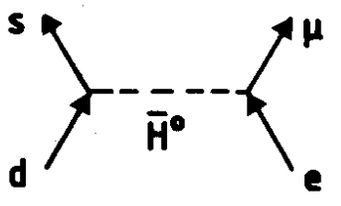

Fig. 7

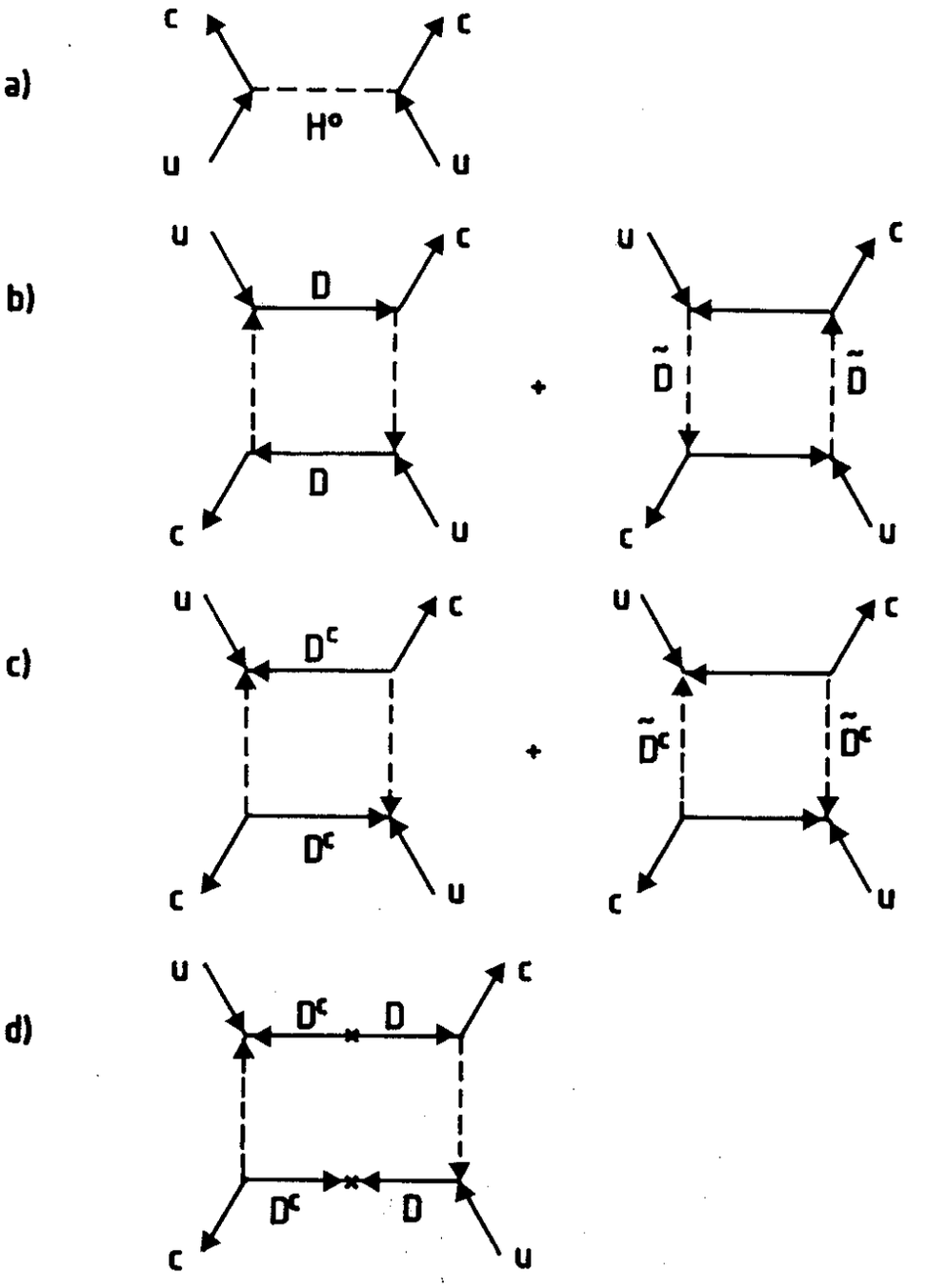

Fig. 8

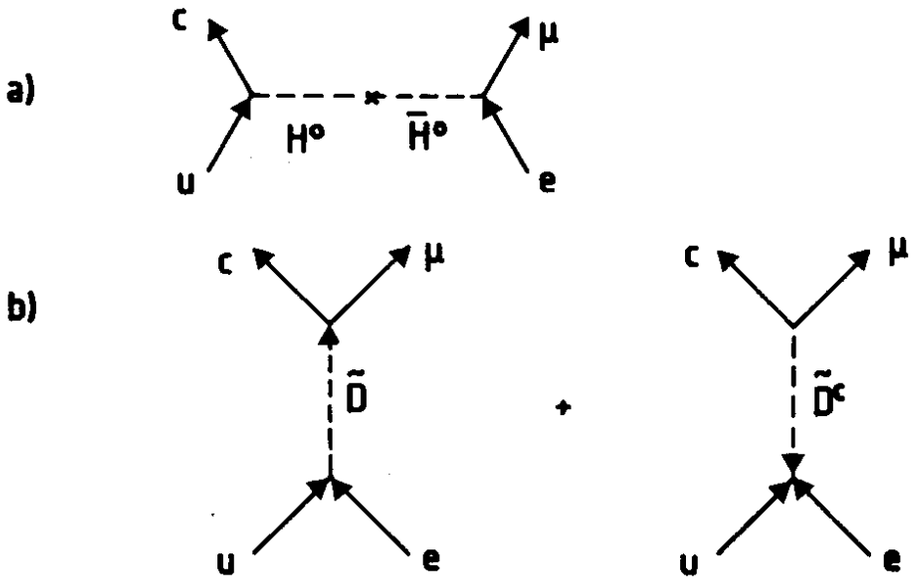

Fig. 9

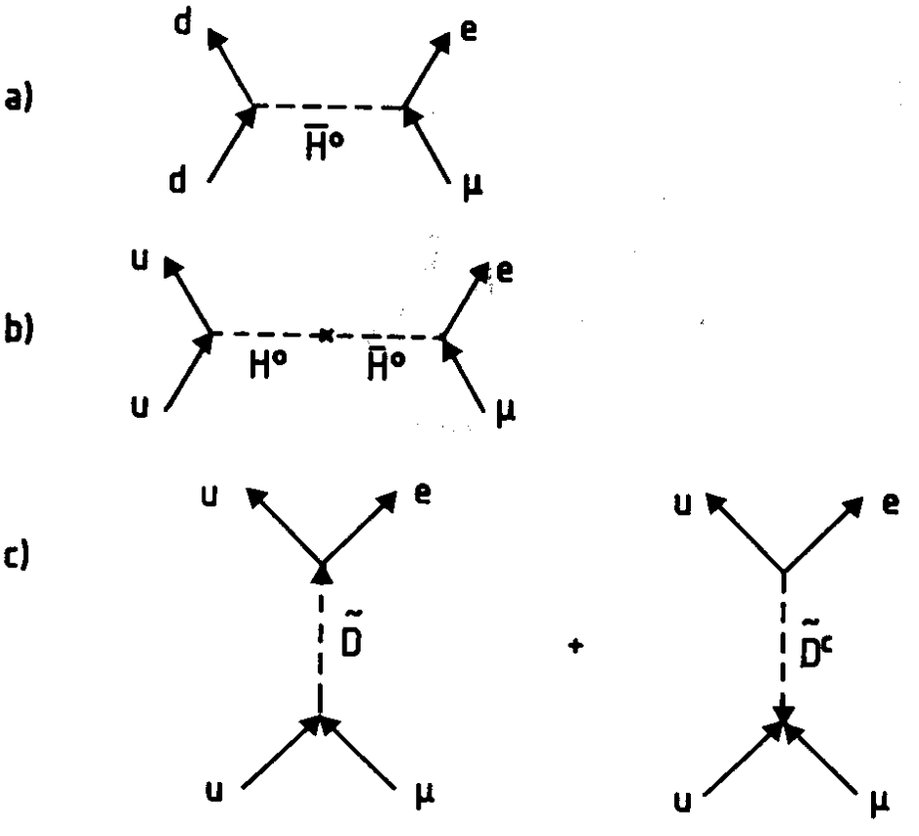

Fig. 10

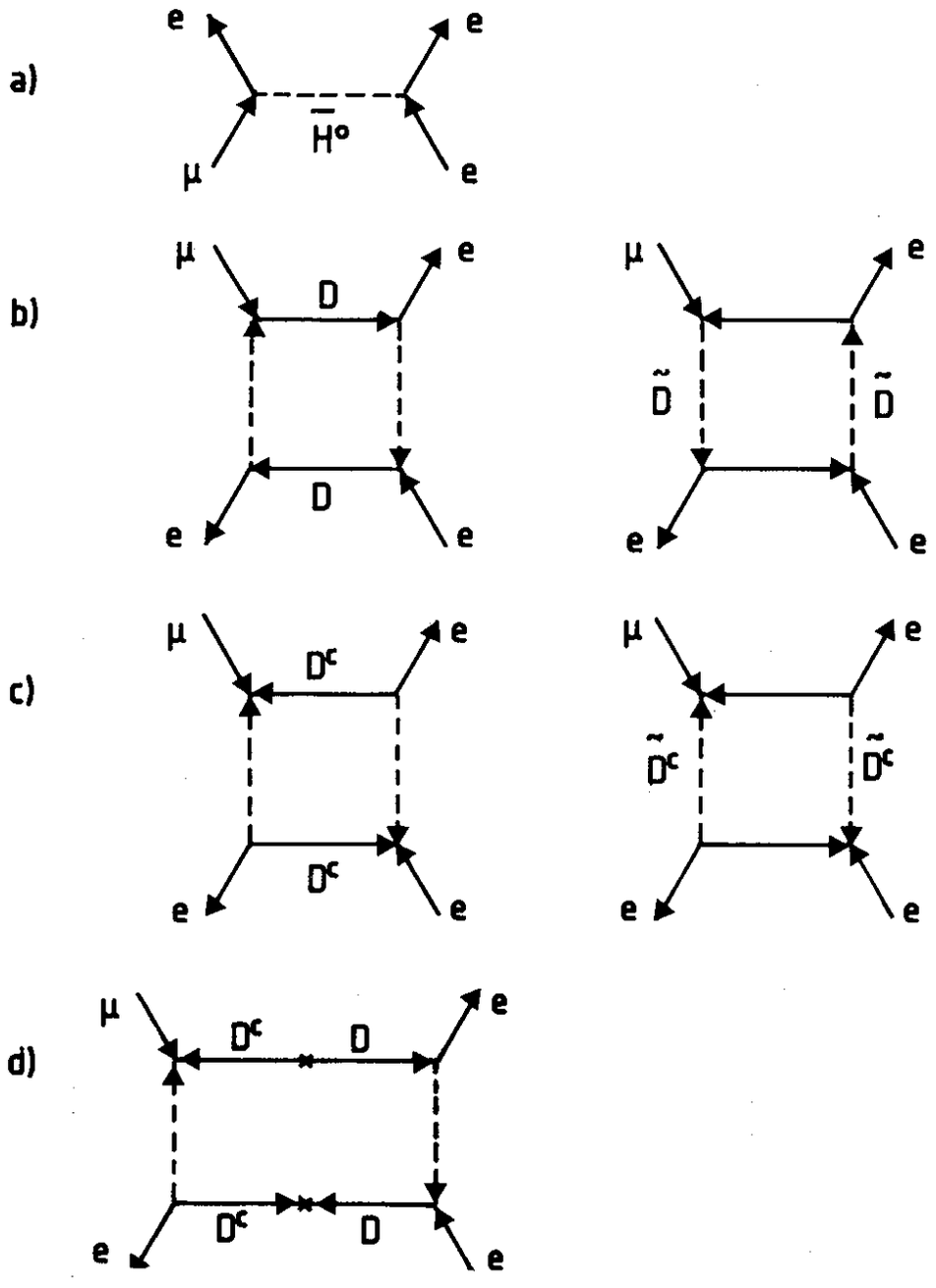

Fig. 11

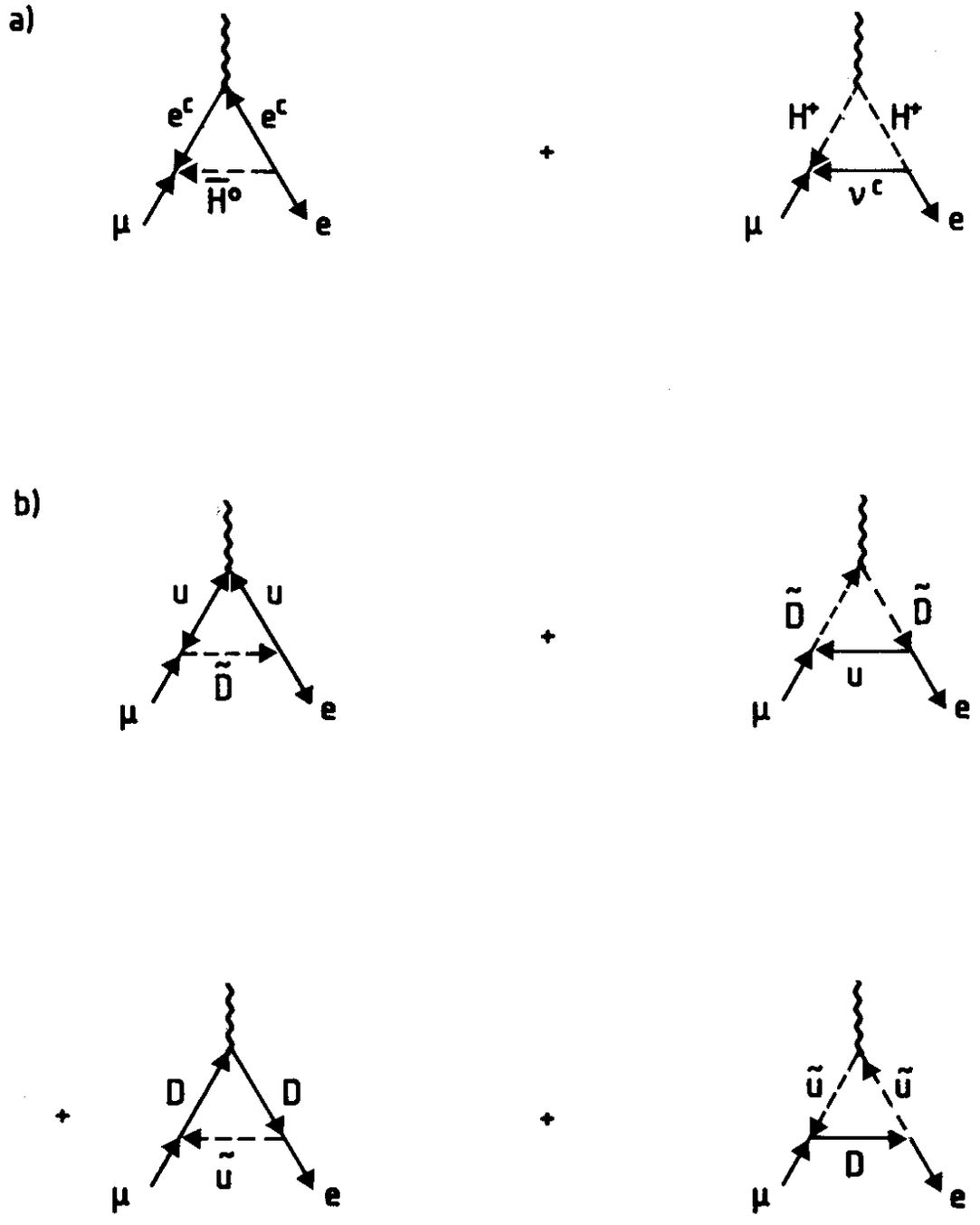
a)
e^c
e^c
$\bar{H}^o$
μ
e
+
H^+
H^+
ν^c
μ
e
b)
u
u
$\tilde{D}$
μ
e
+
$\tilde{D}$
$\tilde{D}$
u
μ
e
+
D
D
$\tilde{u}$
μ
e
+
$\tilde{u}$
$\tilde{u}$
D
μ
e
+ (similar diagrams for D^c)
c)
u
u
u^c
$\tilde{D}^c$
$\tilde{D}$
μ
e

Fig. 12

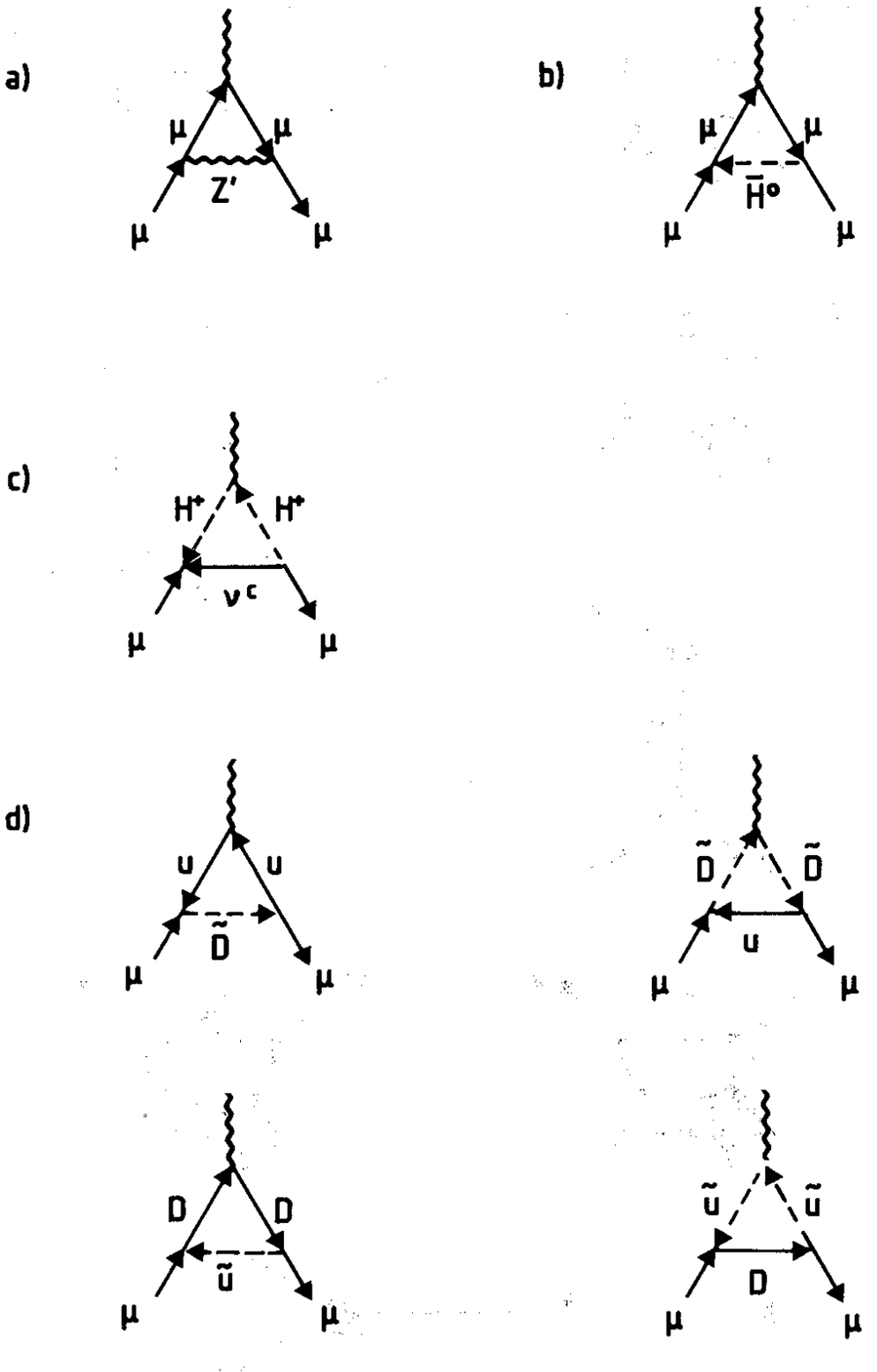

+ (similar diagrams for D^c)

Fig. 13

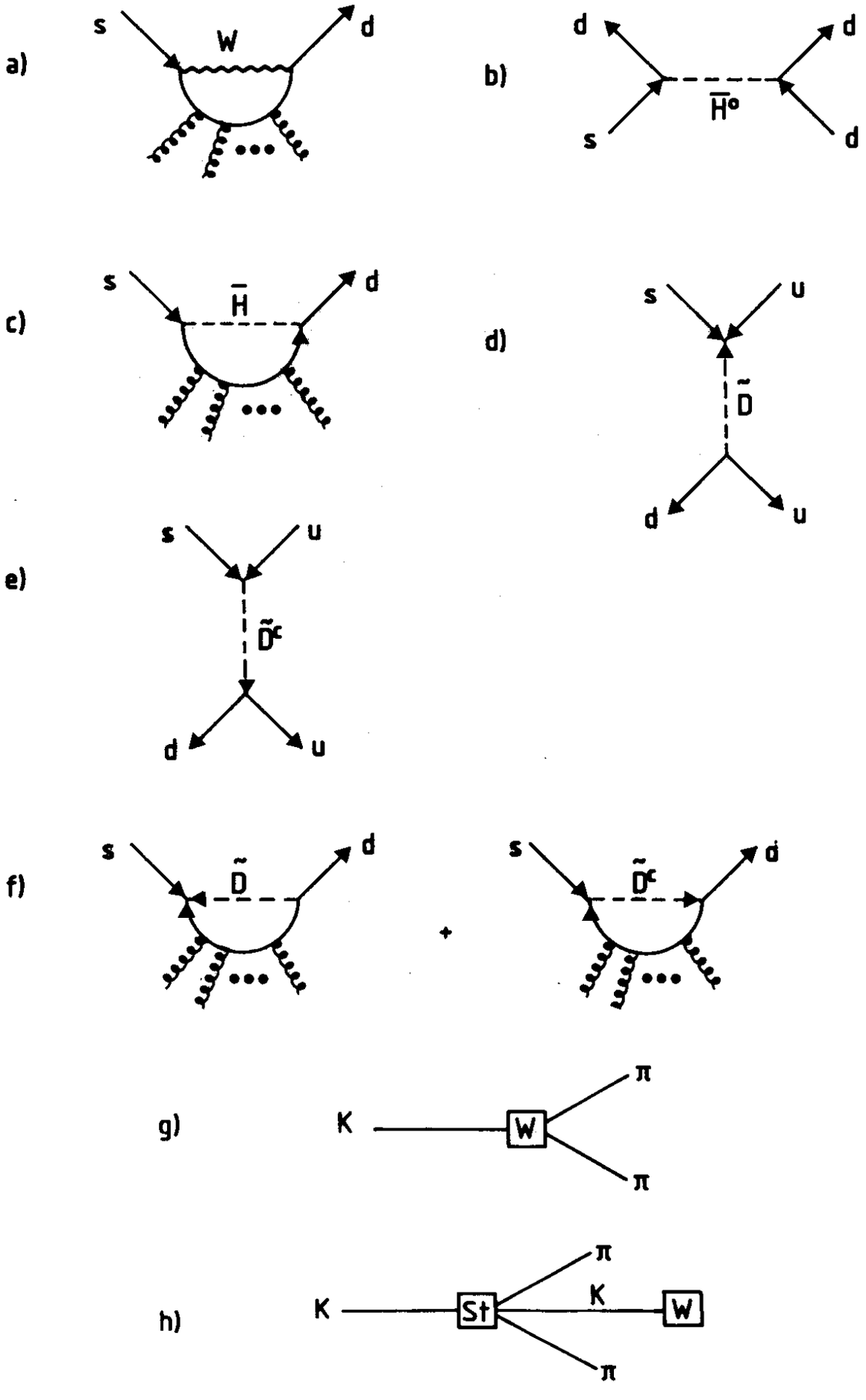

Fig. 14

a)

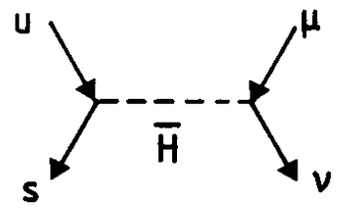

b)

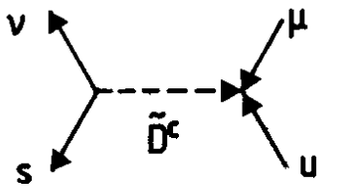

c)

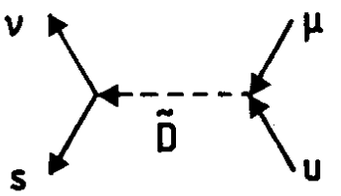

d)

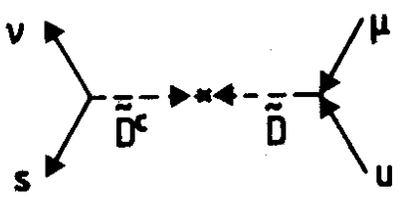

Fig. 15

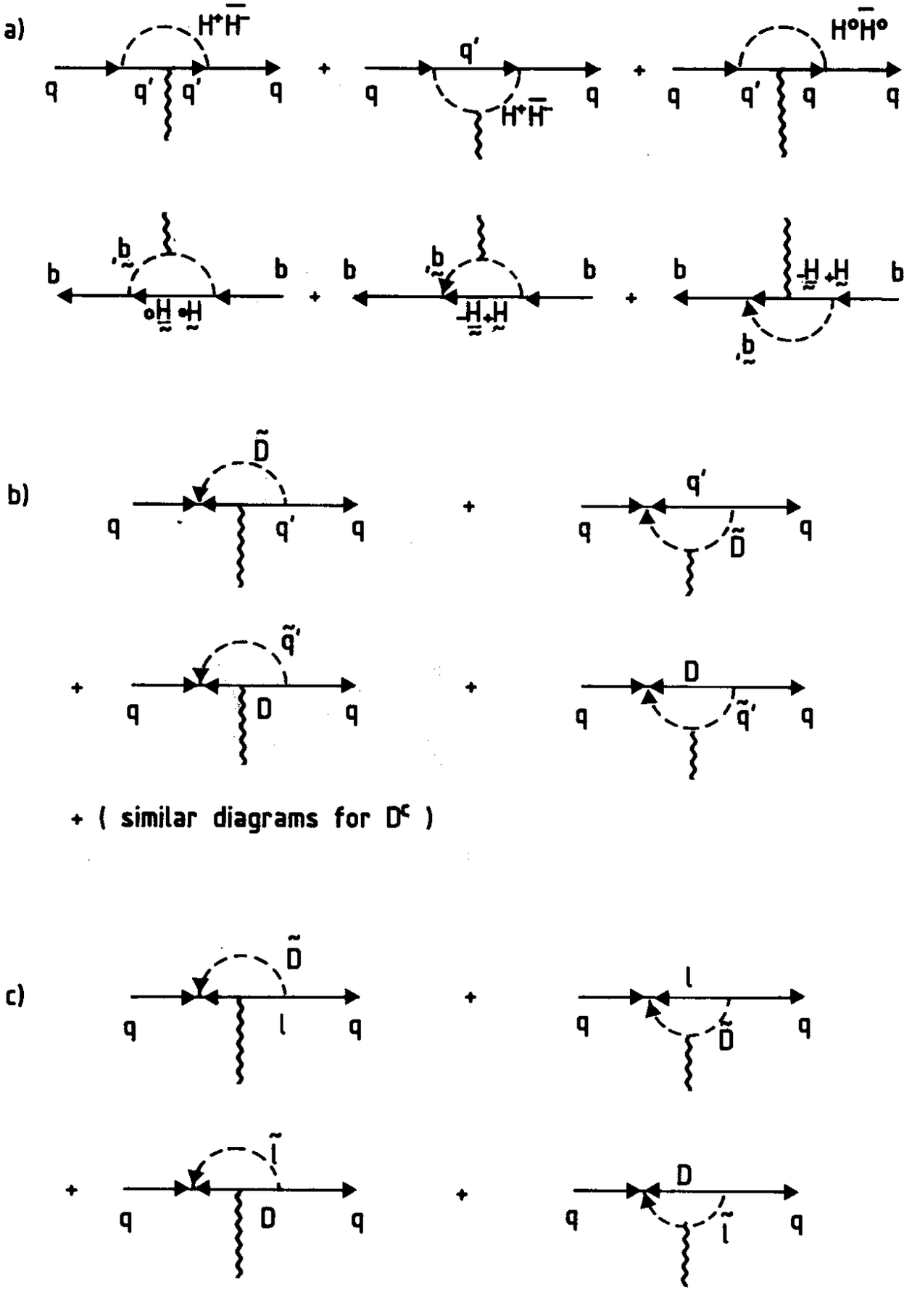

Fig. 16

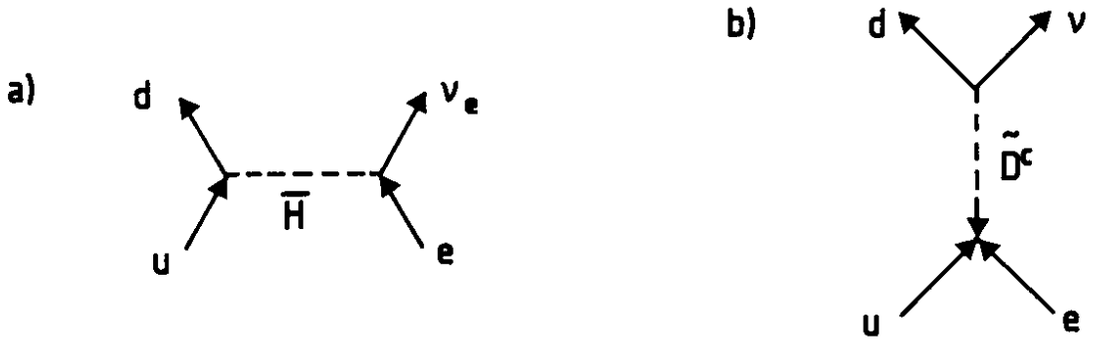
a)
d
ν_e
$\bar{H}$
u
e
b)
d
ν
$\tilde{D}^c$
u
e

Fig. 17

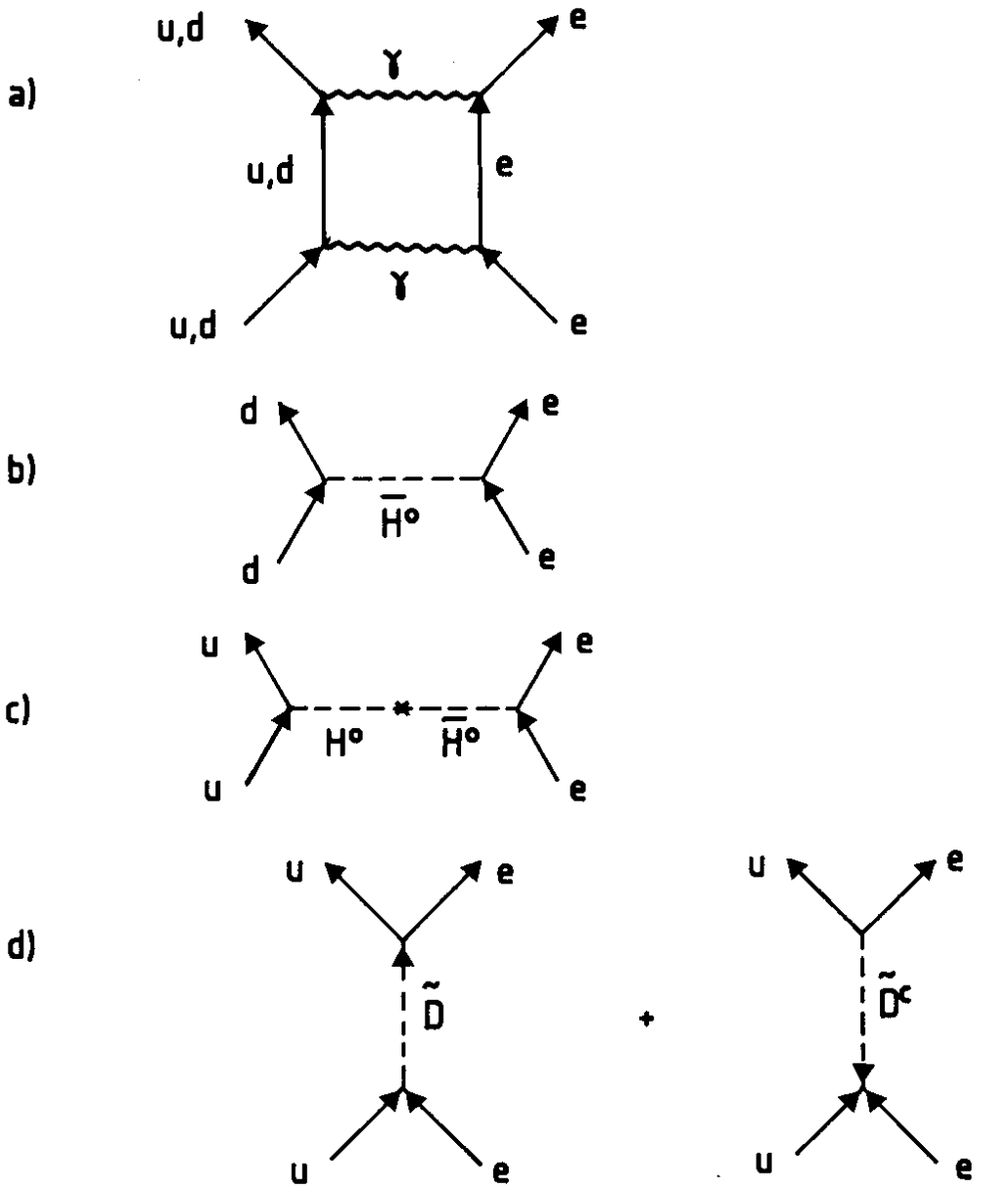
a)
u,d
e
γ
u,d
e
γ
u,d
e
b)
d
e
$\bar{H}^o$
d
e
c)
u
e
H^o
$\bar{H}^o$
u
e
d)
u
e
$\tilde{D}$
u
e
+
u
e
$\tilde{D}^c$
u
e

Fig. 18